

# Macroscale Biomolecular Electronics and Ionics

Nadav Amdursky,\* Eric Daniel Głowacki, and Paul Meredith

The conduction of ions and electrons over multiple length scales is central to the processes that drive the biological world. The multidisciplinary attempts to elucidate the physics and chemistry of electron, proton, and ion transfer in biological charge transfer have focused primarily on the nano- and microscales. However, recently significant progress has been made on biomolecular materials that can support ion and electron currents over millimeters if not centimeters. Likewise, similar transport phenomena in organic semiconductors and ionics have led to new innovations in a wide variety of applications from energy generation and storage to displays and bioelectronics. Here, the underlying principles of conduction on the macroscale in biomolecular materials are discussed, highlighting recent examples, and particularly the establishment of accurate structure–property relationships to guide rationale material and device design. The technological viability of biomolecular electronics and ionics is also discussed.

specifically, changes in membrane potential “move” along neurons which are controlled by the opening and closing of voltage-gated ion channels. Decades of modern biophysical studies have resulted in detailed pathways of electron transport (ET) in biological systems, such as those involved in photosynthesis or in aerobic respiration. As described below, and unlike the conduction mechanisms that play in metals or semiconductors, electron (and indeed ion) flows are mediated in biological systems by mechanisms that involve redox events from a reduced donor to an oxidized acceptor. The spatial organization of the redox centers is directed by proteins, where the redox center is usually a protein’s cofactor, hence the medium between the donor and acceptor redox sites is the protein structure. The observa-

## 1. Introduction

### 1.1. From Electron Transport in Biology to Bioelectronics

In 1791, the Italian philosopher, physicist, and nascent physiologist Luigi Galvani gave birth to the concept of “biological electricity.” In a now famous experiment, Galvani observed the twitching of a dissected frog’s leg upon the application of a potential difference generated from lightning rods. We now understand this observation in terms of the hypothesis that neurons use electrical currents to pass signals to muscles—

tion that electron flows can be mediated within proteins<sup>[1]</sup> led to the emergence of a subfield in bioelectronics in the early 2000s,<sup>[2–4]</sup> where proteins and peptides were examined for their electrical conductance in a molecular junction configuration.<sup>[5,6]</sup> Likewise, DNA has been proposed as a candidate for low-cost sequence programmable nanometer-scale molecular devices.<sup>[7]</sup> Unlike proteins, DNA has no fundamental role in biological ET that we know of, so there have always remained lingering doubts as to whether it is a true “biological conductor.” In addition, the concept of DNA electronics is plagued by reproducibility issues with reported resistances ranging from highly insulating<sup>[8,9]</sup> ( $>10^{13} \Omega$ ) to highly conducting<sup>[10]</sup> ( $<10^4 \Omega$ ). In a direct analogy to the persuasive promises of molecular electronics using synthetic organic materials, biomolecular electronics has likewise attracted visionaries seeking to build complex circuits with DNA, proteins, etc.<sup>[11]</sup> However, this vision is still considered as a pure scientific curiosity rather than a real roadmap toward commercial realization, and we still have much to learn concerning electrical processes at molecular- and macroscales.


The emergence of modern studies on conducting biomolecules in molecular junction configurations was motivated to better understand ET process—many of these studies were performed in solution. Likewise, nanometer-scale electrical processes in synthetic conducting polymers have also utilized molecular junction architectures but more so in the solid state and motivated by the ideas of next-generation electronics and optoelectronics. With a few notable exceptions that we will highlight below (particularly the work of early pioneers such as Rosenberg and co-workers<sup>[12–14]</sup> and McGinness<sup>[15,16]</sup> in the 1960s and 1970s), the concept of “long-range conduction” (micrometers or even millimeters) in biomolecules is a

Dr. N. Amdursky  
Schulich Faculty of Chemistry  
Technion–Israel Institute of Technology  
Haifa 3200003, Israel  
E-mail: amdursky@technion.ac.il

Dr. E. D. Głowacki  
Laboratory of Organic Electronics  
Department of Science and Technology  
Linköping University  
Bredgatan 33, SE-60174, Norrköping, Sweden

Dr. E. D. Głowacki  
Wallenberg Centre for Molecular Medicine  
Linköping University  
58183 Linköping, Sweden

Prof. P. Meredith  
Department of Physics  
Swansea University  
Singleton Park, Swansea SA2 8PP, Wales, UK

 The ORCID identification number(s) for the author(s) of this article can be found under <https://doi.org/10.1002/adma.201802221>.

DOI: 10.1002/adma.201802221

much more recent phenomena of the last decade. A significant example includes  $>\mu\text{m}$  scale conduction along bacterial nanowires.<sup>[17–23]</sup> The underlying mechanism of conduction is still debatable (although considered electronic in nature), but several groups have already showed low resistivity values ( $\approx 1\text{--}20\ \Omega\ \text{cm}$ ) for individual bacterial nanowires in electrical junctions,<sup>[21,24]</sup> with a carrier mobility of  $\approx 0.1\ \text{cm}^2\ \text{V}^{-1}\ \text{s}^{-1}$ .<sup>[22]</sup> Inspired by this extraordinary long-range ET across the bacterial nanowire, a new question arises, can biomolecules be used for the formation of electron or indeed ion conducting biopolymers for use particularly in bioelectronics? This question is the underlying motivation for this review.

## 1.2. The First Observations of Macroscopic Solid-State Conduction in Biomolecules—Melanin as the Case Example

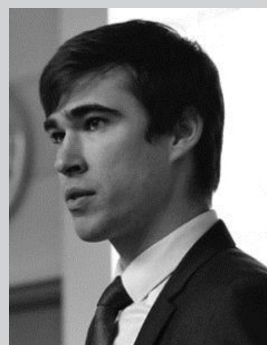
Among early “model” systems to explore solid-state biological conductors was the ubiquitous pigmentary system melanin,<sup>[25–27]</sup> more specifically the brown-black pigment eumelanin. Interest in these indolic macromolecules was stimulated by the theoretical work of Pullman and Pullman<sup>[28]</sup> using some of the first quantum chemical constructs. They suggested that the indolic backbone structure and accompanying electronic delocalization could confer “semiconducting properties”—at the time a very bold hypothesis. The first experimental observations of electrical and photoconductivity in condensed phase eumelanin were made in the late 1960s utilizing simple pressed powder pellets and foil contacts. Potts and Au<sup>[29]</sup> were the first to report photoconductivity, and notable early reports of simple dark-DC conductivity include those by Trukhan et al.,<sup>[30]</sup> Rosenberg and Postow,<sup>[31]</sup> and Powell and Rosenberg.<sup>[32]</sup> The latter authors demonstrated a key feature of eumelanin conductivity—its dependence upon the hydration state (i.e., water content) of the sample: but all conduction hypotheses were based upon electron–hole transport. The hydration-dependent behavior was variously ascribed to arise from a local modification of the dielectric constant by the adsorbed water, lowering the activation barrier for hopping. This proposition was advanced by Rosenberg and co-workers as a generic mechanism to explain the phenomena in all hygroscopic “biological semiconductors.”<sup>[31,32]</sup>

The concept of semiconductivity in melanin was apparently “cemented” into early accepted wisdom by two landmark papers published in 1972 and 1974 by McGinness et al.<sup>[15,16]</sup> In particular, they suggested that the relatively new theories of Mott, Davies, and others concerning the mesoscopic physics of highly disordered inorganic semiconductors could be translated to biological conductors. This was underpinned by observations that pellets of natural and synthetic melanin could reversibly switch between two resistive states with the application of an electric field. They interpreted this as yet more evidence for the amorphous semiconductor model. This reversible switch is arguably the first modern bioelectronic device, and the experimental equipment is housed in the Smithsonian Chip collection in due deference to the discovery. However, and as discussed in greater detail later in the review, several decades of apparently confirmatory semiconductor studies<sup>[33–39]</sup> have been most recently challenged and in some senses debunked,



**Nadav Amdursky** received his Ph.D. degree from Tel Aviv University under the guidance of Profs. Ehud Gazit and Gil Rosenman. He completed his postdocs with Profs. David Cahen and Mudi Sheves in the Weizmann Institute and Prof. Molly Stevens in Imperial College London. Since 2016, he has been an Assistant

Professor in the Technion–Israel Institute of Technology, Schulich Faculty of Chemistry. His research topics include charge transfer across biological materials, bioelectronic devices, and excited-state processes.



**Eric Daniel Głowacki** studied chemistry at the University of Rochester, supervised by Ching W. Tang. He received his Ph.D. degree under the guidance of Serdar Sariciftci and Siegfried Bauer at the Johannes Kepler University in Linz, Austria. In 2015, he was appointed Assistant Professor of physical chemistry in Linz. Since 2016, he has been

affiliated with Linköping University in Sweden as a Wallenberg Center for Molecular Medicine fellow. His research group focuses on nanoscale organic materials for bioelectronics and photochemistry applications.



**Paul Meredith** is a Professor of physics at Swansea University in the UK and holds a Sêr Cymru II Research Chair. He is also an Honorary Professor at the University of Queensland where he was formally an Australian Research Council Discovery Outstanding Researcher Award Professorial Fellow, and Director of UQ Solar

and the Centre for Organic Photonics and Electronics. His research interests focus on next-generation materials for applications including optoelectronics, solar energy, and bioelectronics.

by new evidence showing melanin to be predominantly a protonic conductor.<sup>[25,27,40]</sup> This example highlights the difficulty in isolating and quantifying seemingly very different “current-carrying physics” in biological conductors—a concept that is now firmly embedded at the heart of modern bioelectronics as we seek to transduce between ionic biological signals and

modern semiconductor-based electronic processing. The melanin story is also an archetype of the more recent “DNA-debate” and questions as to whether proteins, lipids, polysaccharides, etc., can intrinsically sustain electronic conduction and hence ET in the solid state.<sup>[13,31,32,41]</sup> That said, it is now appropriate and timely to introduce the basic concepts of ionic conduction.

### 1.3. Short Introduction to Ionic Conductors

As eluded to above, the physics of ionic and electronic currents are quite different, yet can seemingly collide in biological conductors. The field of solid-state ionic conductors (SSICs) has a rich history dating back to the 1830s with the work of Michael Faraday on solid electrolytes. A second group of SSICs was introduced in early 1880s, termed ionic glasses, but it has taken nearly a century to make substantial progress with these materials. 1967 is considered as the actual “birth year” of the solid-state ionics field,<sup>[42]</sup> with the discovery of highly conducting ( $0.1 \text{ S cm}^{-1}$ ) silver iodide ( $\text{Ag}^+$  transport) and sodium alumina ( $\text{Na}^+$  transport) at room temperature.<sup>[43,44]</sup> An additional breakthrough that took place at the same time was the development of polymer-based organic SSICs (also referred to as polymer ionomers) by the DuPont company with a material known as Nafion, a proton conductor (the proton being the smallest ion of course). Other polymer-based organic SSICs include an organic framework matrix (such as polyethylene oxide) doped with inorganic electrolytes that were first introduced in 1975.<sup>[45]</sup> The immediate applications for SSICs include batteries, supercapacitors, and fuel cells, i.e., applications where strong ionic transport is needed with very low electron conductivity and low activation energy.<sup>[42]</sup> Though the silver iodide group of inorganic SSICs has the highest measured ionic conductivity as a group, it is lithium iodide with its much lower conductance that was first used as an SSIC battery (made by Wilson Greatbatch) in pacemakers in 1972.<sup>[46]</sup> Lithium was an essential metal in the development of SSIC batteries (including the now ubiquitous Li ion), first conceptualized by Whittingham in 1976,<sup>[47]</sup> and were commercially available from 1991 from Sony. The advantages of organic SSICs lie in their flexibility, low cost, and ease of thin film formation. Nafion as an efficient proton conductor is probably the current best candidate for proton exchange membrane fuel cells (PEMFCs),<sup>[48–51]</sup> and in 2015 we saw their first commercial use in the Toyota Mirai car. In short, it took nearly 150 years since the discovery of SSICs to deliver commercial applications, but in an ever more carbon constrained world they will eventually become vital components across the technology space.

### 1.4. From Ionic Transport in Biology to Biomolecular Polymeric Ionomers

As earlier stated, ET is fundamental in biology. However, at the heart of most signal-carrying events is ionic transport, and especially in the form of ion channels for  $\text{Na}^+$ ,  $\text{K}^+$ , and  $\text{Cl}^-$ , which are the basis for electrical action in neurons and cardiac cells. Proton transport (PT) is also totally fundamental in biology. For instance, the photosynthetic and aerobic respiration

ET reactions are accompanied by PT across transmembrane protein complexes. This in turn is central to the formation of an electrochemical gradient used to create the energetic coin (ATP). A second example is the proton pump activity of many of the rhodopsin family, although some rhodopsins also pump larger ions. Similar to ET, also (directed) ionic transport is mediated by proteins and potentially other functional bio-macromolecules such as melanins. The tendency for biological structures to adsorb water and the presence of groups that can be protonated (as oxo-acids) have promoted studies of PT conductance across natural biological structures in the solid state. This again, as briefly eluded to earlier, has become one of the most interesting aspects of melanin structure–property studies and a clear reason to consider them as bioelectronic materials.<sup>[25,27,40]</sup> Indeed, the vast majority of the works on SSIC across biological structures/polymers has focused on proton conductivity. These studies started in the 1960s, mainly with the seminal work of Barnett Rosenberg (the same Rosenberg responsible for the modified dielectric constant model that motivated Proctor and McGinness) on films of globular proteins (hemoglobin and cytochrome c), fibrous proteins (collagen), lipids (lecithin), DNA, and of course melanin.<sup>[13,14,32]</sup> This extensive and seminal body of work was accompanied by the studies of Eley on dry proteins and DNA,<sup>[52–54]</sup> and Murphy on cellulose, wool, and silk.<sup>[55,56]</sup> In most of this early research it was found that the macroscopic DC conductance across the material increased with water content, which we now recognize as a hallmark for proton conduction. It is also important to note that, as with the melanin case, most studies were motivated by a search for electronic semiconducting properties. However, close inspection of these data with modern insight into disordered semiconductors and solid-state proton transport would lead one to conclude that electronic effects were essentially absent across the board. It would be interesting and potentially history rewriting to apply the same methodologies that have now become part of the melanin structure–property toolbox<sup>[25,27,40]</sup> to these other bio-macromolecules. Indeed, limited recent examples of where this has occurred is covered in more detail in this review.

To conclude these historical and scene-setting introductory remarks: the history of electronic and ionic conducting biomaterials is rich and long. From a biological material perspective, the molecular junction has been the mainstay of architectures for studying ET. Synthetic conducting polymers have provided new impetus to create next-generation electronics and optoelectronics with visions of using biologically derived materials. SSICs have taken over a century to mature into commercial applications, but are now ubiquitous in storage devices. Polymeric ionic conductors have massive potential to radically change this and related technology spaces. The physics of ion and electronic currents are quite different and they collide in hygroscopic biological conductors such as proteins and melanin where PT appears a dominating factor. It is doubtful whether early observations on solid-state macroscopic electrical conduction were actually electronically related, and this history is steadily being written to replace the charge carrier with the proton. In this review we cover recent advances in understanding of both ionic and electronic biomolecular conductors—focusing primarily on long-range transport over micrometers-to-millimeters-to-centimeters. This is a relatively

new and emerging sub-branch of bioelectronics with considerable potential, and we speculate as to possible uses of such materials.

## 2. Basic Considerations for Macroscopic Conduction in Organic and Molecular Solids

The physics of electrical conduction in crystalline inorganic solids is very well understood. In particular, the “transport physics” of semiconductors such as silicon is defined by periodic Hamiltonian that delivers delocalized charge and a bandgap between the valence and conduction bands as the occupancy states of holes and electrons, respectively. The Fermi energy,  $E_f$ , defines if a material is a metal or an insulator—semiconductors really being the limiting case of an insulator with an energy gap ( $E_g$ ) between conducting and nonconducting states of 1–3 eV. This banded description of conduction has questionable relevance to most of the materials covered in this review which as a general rule are “insufficiently periodic” (i.e., too disordered) to define a relevant Hamiltonian. That said, the quest for organic and bio-organic conductors that possess band-like transport is a constant theme in solid-state physics— notable examples being crystalline molecular semiconductors such as pentacene, and the infamous observations of coherent transport in DNA discussed in the main text.<sup>[57]</sup>

Of considerably more relevance, particularly to macroscale electronic and ionic conduction in biomolecular systems, is to take the most fundamental views: that is, the basic conductivity ( $\sigma$ ) equation

$$\sigma = eN\mu \quad (1)$$

where  $N$  is the conducting charge density,  $e$  is the fundamental charge, and  $\mu$  is the mobility of the majority carrier. The basic task in understanding solid-state conduction is understanding  $\sigma$  in terms of  $N$  and  $\mu$  and their inter-relationships. For organic and bio-organic conductors this must be considered in the context of the important physics, namely, the “molecular nature” of organic solids and the resulting localization of conducting states, the interactions of strongly correlated  $\pi$ -electrons in organic semiconductors, structural and energetic disorder, and the possibility of ions to contribute to or even dominate conduction.

An important example of the interplay between  $\sigma$  and  $\mu$  is the case of an amorphous (the limiting case of disorder) semiconductor where transport is dominated by “hopping” between localized states (we discuss a little more about hopping later in the section). The transition between localized and delocalized transport was famously described by Anderson (the Anderson transition) and formalized for amorphous semiconductors by Mott and Davies with the concept of the mobility edge—a tail distribution of states below the nominal conduction band edge. In this case, the conductivity is strongly temperature dependent and given by

$$\sigma = A \exp(-B/T^n) \quad (2)$$

where  $B$  is the activation energy,  $A$  is the pre-exponential factor (related to  $\mu$ ), and  $n$  is an exponent determined by the

temperature. At around room temperature  $n = 1$ , but at low temperatures  $n = 1/4$ . This physics was invoked by McGinness<sup>[15]</sup> in describing melanin as an amorphous semiconductor—Equation (2) predicts certain electrical behavior such as switching between “two resistive states” by lowering the transport activation energy that was apparently observed experimentally. However, as described in later sections, this turned out to be the manifestation of different physics related to contacts and capacitive effects. This is another example of the difficulties of applying standard solid-state physics constructs to complex and heterogeneous biomolecular systems.

An alternative view of the electronic structure of molecules is molecular orbital (MO) theory.<sup>[58]</sup> In the MO construct one can define molecular orbitals for entire molecules (if of course the molecule is well defined in its own right) via a linear combination of atomic orbitals. While a detailed discussion of MO theory is outside the scope of this review, it is worth noting that early activity in studying conduction in DNA was based upon a principle that base pairs had overlapping electronic orbitals that could produce a delocalized MO.<sup>[59]</sup> In addition, although MO theory strictly applies to the development of orbitals on the molecular scale, its concepts have become a central pillar for describing transport and electronics of organic semiconductors through the HOMO–LUMO nomenclature, respectively the highest occupied and lowest unoccupied molecular orbitals, which have somewhat erroneously morphed into direct analogies with the valence and conduction bands of traditional solid-state theory.

However, and more in keeping with the long range or bulk transport scope of this review, we return to the concept of hopping between localized states the dynamics of which are strongly influenced by coupling to the local environment. This is particularly pertinent in the context of biomolecules that often exist, even in the solid state, in a constantly changing potential landscape dominated (for example) by solvent, polarity, etc. The movement of a charge from one site to another induces changes in the local environment and perturbation of molecular structure—or the formation of a polaron. Thus, electronic hopping transport in a biomolecular system is a mix of intrinsic and extrinsic factors, and strongly temperature dependent. The mobility under such circumstances can be described by the simple activation equation

$$\mu = \mu_0 \exp\left(-\frac{E_H}{k_B T}\right) \quad (3)$$

where  $\mu_0$  is a pre-exponential factor and  $E_H$  is the energy barrier average height for a hopping event. As far as we can ascertain, there appears to be no  $\exp(-B/T^{1/4})$  behavior at low temperatures as observed in amorphous semiconductors (see Equation (2)). In this regard, there appears to be a fundamental difference in localized hopping transport between disordered inorganic and molecular materials. This difference and the impact of extrinsic factors on the carrier mobility and free carrier number density are quite fundamental features of electronic conduction in biomolecular solids.

The obvious question arises in considering biomolecular solids: does this electronic transport physics translate to ions, and in particular the limiting case of the proton? The electrical

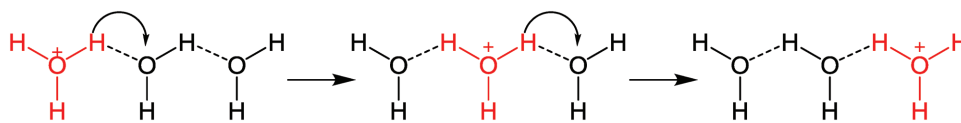


**Figure 1.** The Grotthus mechanism showing how an ionic charge hops through a hydrogen-bonded network. This type of ion transport is highly relevant to hydrated conducting biomolecules.

properties of biomolecular materials are, as described variously here, strongly dependent upon local hydration/solvation conditions. This is not surprising since biological systems are “wet and ionic.” To demonstrate the principles at play in bulk movement of an ionic charge carrier in a biomolecular conductor, we now discuss the example of proton transport in water where there are two basic mechanisms. The first is center-of-mass diffusion known as the “vehicle mechanism.”<sup>[60,61]</sup> In this case, the transport can be simply described by the Einstein–Stokes equation for charged particles

$$\mu = \frac{Dq}{k_B T} \quad (4)$$

where  $D$  is the diffusion constant and  $q$  is the charge. The second possible mechanism is proton tunneling or hopping termed the Grotthus mechanism<sup>[61–63]</sup> as shown schematically in **Figure 1**. The mechanism involves the rapid transfer of an ionic defect through a hydrogen-bonded network. The process is thought to be cooperative, although there is still considerable debate as to how cooperative and whether or not there is any site-to-site coherence. What is clear though is that the polarization and orientation of water molecules (hydrogen bonding) in this chain is critical to facilitating faster transport than simple center-of-mass diffusion.

In a direct analogy to electronic hopping, the transport of an ion through a conducting medium can be represented by

$$\sigma = \frac{A}{T} \exp\left(-\frac{E_A}{k_B T}\right) \quad (5)$$

where  $A$  is a pre-exponent now related to center-of-mass diffusion where the exponential captures a tunneling, heat-activated process with activation energy  $E_A$ . It has been suggested that something akin to a percolation transition exists between the two regimes of center-of-mass diffusion and hopping—for example the existence of a percolated network of water spanning two contacts in a hydrated biomolecular conductor.<sup>[64]</sup> Such a transition would lead to a rapid change in mobility and thus conductivity of the form

$$\sigma \propto H^d \quad (6)$$

where  $H$  is the water content and  $d$  is the critical exponent. Whether this represents a true thermodynamic phase transition is, however, an unresolved question since exact determination of the critical exponent is nigh impossible for the case of a hydrated solid.

The similarity between Equations (2) and (5) makes distinguishing between hopping of proton transport to an electronic p-type transport challenging. At the macroscopic

level, a proton looks very much like a large effective mass hole (a p-type polaron particularly). This has, and will continue, to cause confusion and misassignment especially if the interrelationship between hydration and temperature is not properly accounted for. However, solid-state measurements of ion transport, particularly at DC, are considerably more difficult than the equivalent electronic measurements for one quite simple reason: standard metal electrodes are blocking with respect to protons or ions. Blocking and unblocking contacts in ionic circuits are directly analogous to Ohmic or Schottky concepts in electronics—although a strongly blocking contact is very problematic from a measurement perspective, and more so with large static electric fields. At small-to-moderate fields, injection and extraction rates are approximately equivalent so that the system can appear to be “Ohmic” (linear current–voltage behavior). However, at higher fields the blocking nature of contacts leads to the development of space charge and strong capacitive effects. As such, the DC field dependence of the current becomes non-Ohmic resulting in a Child’s law relation

$$i \propto V^\alpha \quad (7)$$

where  $i$  denotes current and  $V$  is the voltage, and  $\alpha$  is a power. Hence we see that strong sublinear behavior of the current can arise as the contacts become more blocking. It is also true that electronic systems can exhibit Child’s law behavior, so this phenomenon in its own right cannot be used to identify the carrier type. It is therefore most common to use AC impedance methods to study ionic or indeed hybrid-electronic conductors. However, this is by no means a precise science and the definition of an appropriate equivalent circuit and the subsequent semiempirical fitting of circuit elements remains problematic.<sup>[65]</sup> There have been attempts to create Ohmic-proton contacts, most notably hydrogenated palladium that is essentially a solid-state electrochemical electrode. Zhong et al.<sup>[66]</sup> successfully used the approach to create a “protonic field effect transistor” where the conducting channel was a hydrated polysaccharide (maleic-chitosan). They observed proton mobilities of order  $5 \times 10^{-3} \text{ cm}^2 \text{ V}^{-1} \text{ s}^{-1}$ , which is close to that predicted for hopping transport via the vehicle mechanism. Finally, it is worth stressing that macroscale electrical measurements in conducting biomolecules—be they AC or DC—must be understood in the context of the following:

1. The strong effect of extrinsic parameters such as hydration, salt content, solvation, etc.
2. The invariably non-Ohmic nature of contacts and the potential for “electrochemistry” to occur within the potential window of the measurement.
3. The possibility for strong ionic contributions to conduction.
4. The temporal and nonequilibrium nature of the current–

voltage characteristics: the coexistence and relative contributions of injection, extraction, and displacement currents.

This section has highlighted the differences and similarities between electron and ion transport, and these are summarized for clarity and convenience in **Table 1**.

### 3. Biomolecular Electronic Materials at the Macroscale

In this main section of our review, we detail the large variety of biological-origin molecules that have been used for the formation of conductive materials on the macroscopic scale, while differentiating between the different monomers used for the formation of the final material.

#### 3.1. Materials based on Small Biological Molecules

The first section covers the use of relatively small molecules ( $\lesssim 1000$  Da) that can form usually crystalline materials with attractive electronic or ionic conductivity over macroscale distances.

##### 3.1.1. Indigo and Indigoids

Indigos produced in living systems share a similar biosynthetic pathway as melanins, which are discussed in detail in Section 3.2.3. The literature on indigos as natural and synthetic, commercialized colorants is extremely extensive, and spans over two centuries.<sup>[68,69]</sup> In the context of electronics, several natural-origin indigos have proven to be intrinsic

semiconductors, giving ambipolar charge-carrier mobilities in the range from  $10^{-4}$  to  $0.2 \text{ cm}^2 \text{ V}^{-1} \text{ s}^{-1}$ .<sup>[70]</sup> They are also electrochemically active materials suitable for sensor and battery applications. Historically, they have been extracted from plants and animals for centuries to be used as dyes and pigments.<sup>[71]</sup> Indigos have very low solubility in organic solvents and water and are traditionally processed via the vat dyeing method.<sup>[72]</sup> In modern times, chemical reduction with sodium dithionate or electrochemical reduction processes are employed.<sup>[73–75]</sup> Electrochemical reduction can be direct or mediated by a redox shuttle such as glucose.<sup>[75]</sup> These reversible redox properties of indigos foreshadow their ability for ambipolar charge transport. Partially soluble forms of oxidized indigos, so-called dehydroindigos, can also be obtained, but have not been used in dyeing processes. Dehydroindigo has been, however, found to be the colorant in the inorganic composite pigment Maya blue, and likely laponite blue.<sup>[76]</sup> In these materials, the indigo molecules form a hybrid structure with the clay mineral palygorskite.<sup>[77]</sup> The vat dyeing redox chemistry foreshadows the reversible redox chemistry that indigoids can support, an important feature when considering application as an organic electronic component. A significant feature of indigoids is the presence of ultrafast photoinduced proton transfer in the excited state, resulting in rapid ( $<10$  ps) deactivation of the excited state.<sup>[78–81]</sup> Because of this, indigos have very low fluorescence and phosphorescence quantum yields on the order of  $1 \times 10^{-3}$ . The very short lifetime of the excited state means indigoids are not suitable candidates for electronic devices where photocurrent generation or light emission is desired. However, the short excited-state lifetime is implicated as the reason for the outstanding photostability of indigo dyes and pigments. The redox- and photoprocesses general to indigo and its derivatives are schematized in **Figure 2a**. The insolubility of indigo, save in its reduced form, precludes synthetic manipulation and also processing from solution. The solubility issue was overcome in several works by using a protect–deprotect strategy, whereby the NH functional groups of indigo are substituted with solubilizing groups which can later be removed by heat or acid treatment (**Figure 2b**).<sup>[82]</sup> This strategy enables solution processability of indigo-based small molecules and polymers,<sup>[83]</sup> and colloidal nanocrystals.<sup>[84]</sup> Indigo can easily be sulfonated to yield indigodisulfonate, also known as indigo carmine, with good water solubility (**Figure 2c**). The indigo carmine disodium salt, widely deployed as an edible food dye, can be crystallized to give a solid-state electrode suitable for rechargeable lithium<sup>[85]</sup> and sodium<sup>[86]</sup> ion batteries.

The first example of using indigo as an active electronic material was reported by Uehara et al.<sup>[87]</sup> in 1987, where thin films of evaporated indigo between Al and Au electrodes were explored as photovoltaic Schottky diodes. The power conversion efficiency of these devices was found to be very low, on the order of  $10^{-5}\%$ . Indigo was rediscovered and explored in much more detail as an intrinsic semiconductor starting in 2012, with the publication of Irimia-Vladu et al.<sup>[88]</sup> showing ambipolar charge-carrier mobility in indigo thin film transistors. The indigo devices (**Figure 3**) featured biomaterials as the substrate (shellac resin), the dielectric (tetratetracontane wax), and indigo (semiconductor). Thin films of indigo demonstrated mobility of  $10^{-2} \text{ cm}^2 \text{ V}^{-1} \text{ s}^{-1}$  and operational

**Table 1.** A summary of the different charge transport properties of ions and electrons in relation to conducting biomolecular solids.<sup>[41,52,58,67]</sup>

Ionic physics	Property	Electronic physics
Center of mass diffusion (vehicle)	Charge transport mechanism	QM tunneling
Site-to-site hopping (Grotthuss)		Hopping between localized states
$<10^{-2} \text{ cm}^2 \text{ V}^{-1} \text{ s}^{-1}$	Charge carrier mobility ( $\mu$ )	Semiconductors:
Hopping: $\mu \propto -E/kT$		$<10^3 \text{ cm}^2 \text{ V}^{-1} \text{ s}^{-1}$
Free carriers: $\sigma = n\mu q$	Electrical conductivity ( $\sigma$ )	Hopping: $\mu \propto -E/kT$
		Free carriers: $\sigma = n\mu e$
kHz (ms carrier transit times)	Maximum device switching rates	GHz (ns carrier transit times)
Inter- or intramolecular (chemical)	Trapping	Localized states within the gap
Liquid: no issues (electrochemical)	Contacts	Ohmic, Schottky,
Solid state: problematic, mostly blocking—gels, ionic, and $\text{PdH}_x$		blocking or transparent, and electron or hole
Ice, acids, bases, Nafion, PEDOT:PSS, polyelectrolytes, bio-macromolecules, and organohalide perovskites	Solid-state examples	Inorganic and elemental semiconductors, quantum dots, organic semiconductors, PEDOT-PSS, and organohalide perovskites

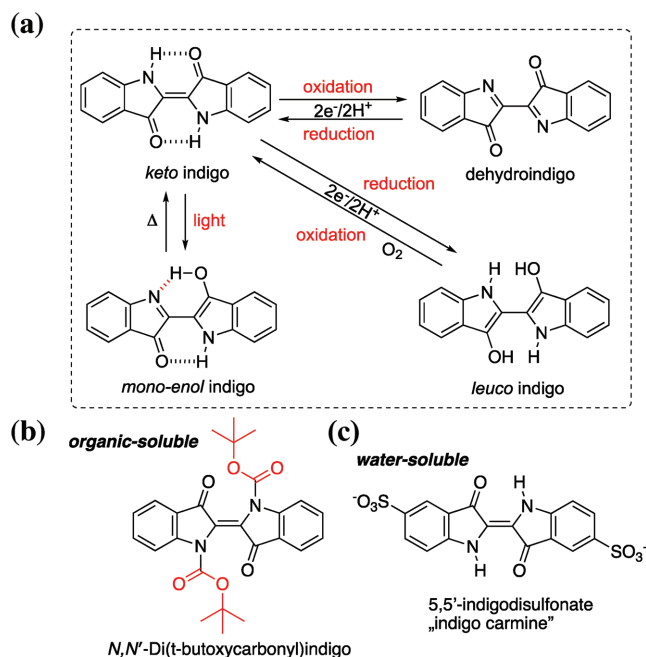


**Figure 2.** a) The (photo)redox properties of indigo, showing the reduced and oxidized forms of indigo and the photoinduced proton transfer reaction to form the transient mono-enol tautomer. b) Organic-solvent soluble indigos can easily be obtained by attaching *t*-butoxycarbonyl (tBOC) functional groups to the NH functional group of indigo. These tBOC protecting groups eliminate the possibility of hydrogen bonding. The tBOC functional group can easily be removed via the action of strong acid, base, or by heating. c) Direct sulfonation of indigo yields indigo carmine and its various salts.

stability in air. Ambipolarity in transistor geometry is easy to observe due to the low bandgap of indigos (indigo  $E_g = 1.65$  eV) allowing carrier injection from a single metal electrode, such as gold.<sup>[89]</sup> Better air stability and high mobility was found for 6,6'-dibromoindigo, the famous tyrian purple dye of animal origin.<sup>[90,91]</sup> The semiconducting behavior of indigos is closely correlated with their crystalline structure, with a common theme of hydrogen bonds creating a hydrogen-bonded polymer of indigos along one crystallographic axis

(Figure 4a), while  $\pi$ - $\pi$  stacking exists along one or two of the other axes (Figure 4b). Various substituents affect the  $\pi$ - $\pi$  stacking intermolecular distances, with closer packing corresponding roughly to higher mobility.<sup>[92]</sup> Orientation of the  $\pi$ - $\pi$  axis parallel to the gate electrode is critical for observing high mobilities. Inducing this “standing” orientation of indigo molecules can be achieved by using low surface-energy aliphatic gate dielectric modification layers.<sup>[70,93]</sup> The crystal structures of indigo and tyrian purple are thoroughly characterized, including thin-film polymorphism.<sup>[94,95]</sup> Growing large single crystals of indigo and its derivatives has proven to be straightforward, most commonly via sublimation. This has made understanding the semiconducting behavior of indigos in the solid state more facile than in the case of less defined or more heterogeneous bioorganic conductors discussed within this review. On top of several naturally occurring indigos, a number of synthetic derivatives of indigo have been tested for their performance in thin film transistor geometry, giving mobility in a similar range, and good stability.<sup>[89,92,93]</sup> While all naturally occurring indigos, according to published reports, pack with the “criss-cross” lattice with each molecule forming single hydrogen bonds to four neighbors, some synthetic indigos such as 6,6'-dichloroindigo and 6,6'-dithienylindigo form linear hydrogen-bonded chains and an idealized brick-wall lattice (Figure 4c).<sup>[83]</sup> The extended dibenzoindigo<sup>[96]</sup> likewise forms hydrogen-bonded chains with a staircase pattern, reminiscent of hydrogen-bonded pigment quinacridone.<sup>[97]</sup> An isomer of indigo, epindolidione, can be formed by thermal isomerization of indigo at 460 °C. Epindolidione forms hydrogen-bonded linear chains and gives mobility up to  $1 \text{ cm}^2 \text{ V}^{-1} \text{ s}^{-1}$  and stable photocatalytic properties in aqueous environments.<sup>[98,99]</sup> Throughout these works, indigo and its derivatives were processed by vacuum sublimation due to the prohibitively low solubility of indigo in organic solvents. Despite the fundamental characterization of indigo as a stable ambipolar semiconductor, its application in practical electronics and bioelectronics remains to be realized. Limited processability of indigos remains an obstacle, however in terms of its electronic properties, it is the highest-mobility material of natural origin, and it has proven nontoxicity and biodegradability.

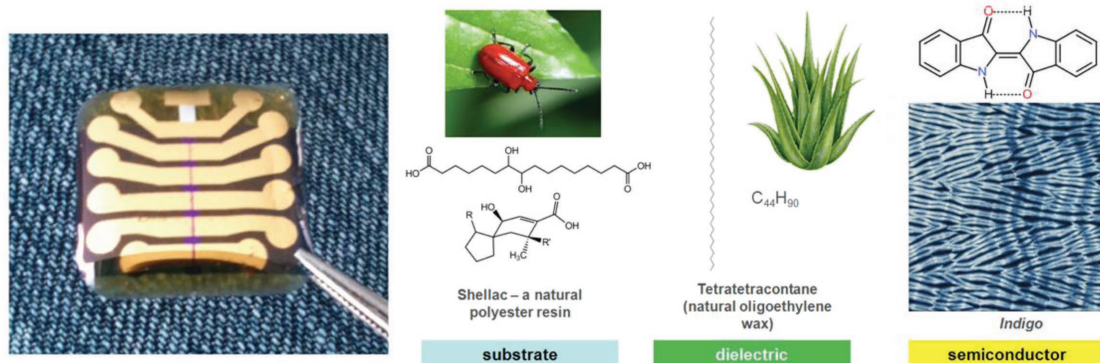


**Figure 3.** Indigo transistors and circuits fabricated entirely of natural-origin materials. The photograph on the left shows an array of indigo thin-film transistors fabricated on a shellac substrate, using a gate dielectric layer of tetratetracontane. The tetratetracontane layer is a hydrophobic low surface-energy material which induces a “standing” orientation in the growth of the indigo molecules, which aligns the  $\pi$ - $\pi$  stacking parallel to position of the source–drain electrodes. This molecular alignment is critical for observing charge transport in indigo layers.

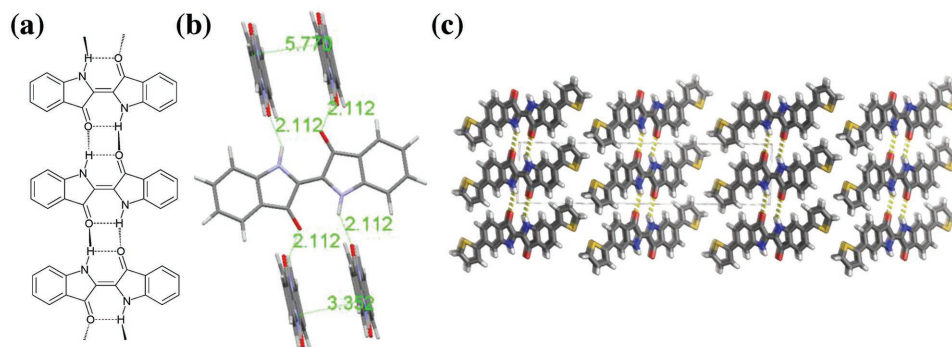


**Figure 4.** Indigo solid-state structure. a) Hydrogen bonding between amine hydrogens and carbonyl groups is the dominant intermolecular interaction governing the crystallization of indigo. The indigo molecules arrange in a criss-cross hydrogen-bonded polymer, where b) each indigo molecule forms single hydrogen bonds with four neighbors. This produces a cofacial  $\pi$ - $\pi$  stacking arrangement along the crystallographic axis that is orthogonal to the hydrogen bonding. c) A few indigo derivatives such as the synthetic 6,6'-dithienylindigo arrange in linear-chain hydrogen-bonded polymers, where each molecule forms double hydrogen bonds to two neighbors.

### 3.1.2. Carotenoids

This class of organic pigments has the general structure of polyene chains consisting of repeating isoprene units, giving a total of 9–11 conjugated bonds. Carotenoids play numerous roles in natural photosynthetic processes as they have light-harvesting, energy-transferring, and photoprotective functions. These photophysical functions are mediated by the complex low-lying singlet-excited-states in carotenoids. In particular, the all-trans conjugated chain with  $C_{2h}$  symmetry gives rise to low-lying singlet states, including the optically allowed  $S_2$  ( $1B_u^+$ ) and the optically forbidden  $S_1$  ( $2A_g^-$ ),  $1B_u^-$ , and  $3A_g^-$  states, concerning transitions from/to the ground  $S_0$  ( $1A_g^-$ ) state. The fundamental photophysics of this complex system has been a topic of extensive study in the ultrafast photophysics community. The amount of attention given to potential electronic transport properties of carotenoids has been much smaller. It was recognized that carotenoids resemble the idealized conducting polymer polyacetylene, and they are indeed an oligomeric form of this polymer. Upon charge-transfer doping, a polyene favorably stores charge in pairs of spatially delocalized charged solitons, which repel one another. The question is whether the limited amount of double bond repeat units of carotene can accommodate stable dications or rather only allow the formation of single radical species. Electron paramagnetic resonance and infrared vibrational spectroscopy corroborate that upon oxidative chemical doping, spinless charged solitons form on  $\beta$ -carotene (the most studied representative carotenoid, **Figure 5a**).<sup>[100]</sup> Solitons are a form of charge storage unique to polyene conjugated systems, confirming the analogous nature of carotene to its larger relative polyacetylene. Electrical conductivity was not directly evaluated in this study. Processed into thin films from chloroform solution,  $\beta$ -carotene demonstrated p-type mobility of  $4 \times 10^{-4} \text{ cm}^2 \text{ V}^{-1} \text{ s}^{-1}$  in transistors. These devices featured a gate dielectric made of glucose thin films, on edible substrates such as gelatin, representing the first example of a field effect transistor (FET) device fabricated entirely by naturally occurring materials (**Figure 5b**).<sup>[101,102]</sup> Operational stability was a problem since carotene easily oxidizes and degrades.<sup>[103]</sup> The p-type nature of  $\beta$ -carotene was confirmed in a study of heterojunction diodes between

n-type Si and carotene.<sup>[104]</sup> Organic photovoltaics employing spin-coated  $\beta$ -carotene layers were reported in 2011, using fullerene or indigo as electron-acceptor layer. The formation of a successful donor-acceptor heterojunction was confirmed by comparing the photocurrent of device with acceptors being at least 2 orders of magnitude higher than diodes with a neat film of  $\beta$ -carotene.<sup>[103]</sup> The carotenoids  $\beta$ -carotene, fucoxanthin, and lycopene (red color of tomatoes) were explored as p-type electron donors in bulk heterojunction donor-acceptor solar cells, using fullerene derivatives as acceptors.<sup>[105]</sup> This study also estimated the mobility of thin films of lycopene, finding a hole mobility of  $2.1 \times 10^{-2} \text{ cm}^2 \text{ V}^{-1} \text{ s}^{-1}$ , significantly higher than  $\beta$ -carotene and fucoxanthin. This resulted in lycopene giving the best performance in the solar cells. Nevertheless, power conversion efficiencies of these devices remained below 0.5%. Zhuang et al. took this concept a step further by utilizing lycopene as electron donor and natural chlorophylls as acceptors (**Figure 5c**). Power conversion efficiency remained below 0.1%, however with open-circuit voltages up to 800 mV.<sup>[106]</sup> An obstacle encountered by researchers is the inherent instability of carotenoids to oxidation. The instability of carotenoids with respect to oxidation has been argued and could be a potential advantage of these materials for deployment in “transient” biodegradable or resorbable electronics.

### 3.1.3. Photosynthetic Porphyrins

Porphyrins are naturally occurring dye macrocycles with an aromatic 18  $\pi$ -electron conjugated system. They fulfill important roles in a diversity of biological processes, including cellular respiration, mediation of reactive oxygen species, detoxification of xenobiotics, transport of oxygen, fatty acid oxidation, and light harvesting. The strong visible-light absorbing property of this chromophore is enriched by the ability of the four pyrrole rings that constitute porphyrin to chelate metals, which results in additional absorption bands. The central role of porphyrins in natural photosynthesis has inspired many researchers to apply natural porphyrins, specifically chlorophyll-a, as photovoltaic materials. During the boom in semiconductor research following the Second World War, many attempted to consider



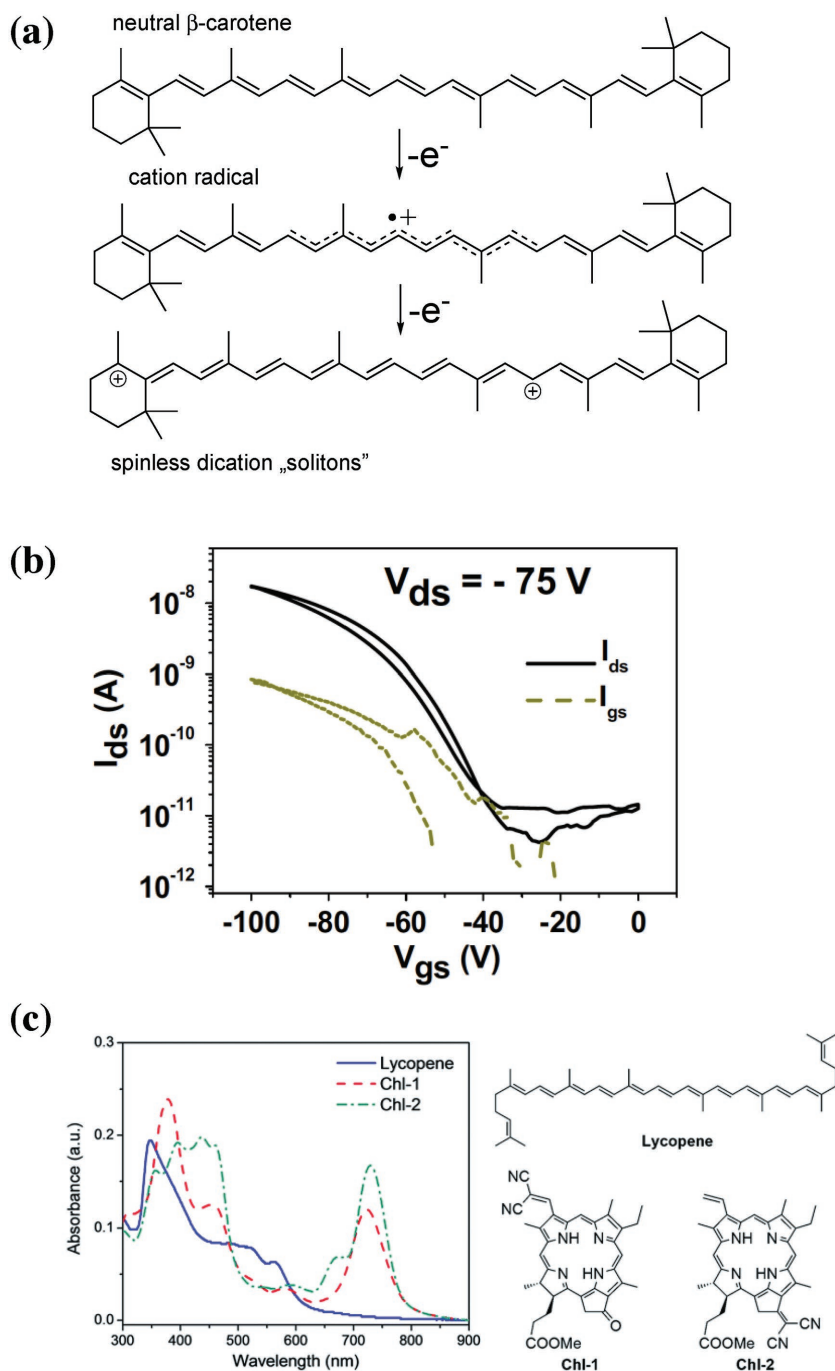


**Figure 5.** a)  $\beta$ -Carotene is a representative polyene system which, upon oxidative doping, favorably stores charge in the form of spinless dication “solitons” as opposed to radical cations. b) Transfer characteristic for a thin-film transistor employing spin-coated  $\beta$ -carotene as the semiconductor layer. The  $\beta$ -carotene demonstrates p-type transport with a mobility  $\mu_h = 4 \times 10^{-4} \text{ cm}^2 \text{ V}^{-1} \text{ s}^{-1}$ . b) Reproduced with permission.<sup>[101]</sup> Copyright 2010, Elsevier. c) Heterojunction solar cells have been fabricated with lycopene as the electron donor and chlorophylls (discussed in detail in Section 3.1.3) as the electron acceptors. The absorbance plot shows the optical density of a 20 nm thick film of lycopene as well as the two chlorophylls used in fabrication of the solar cell. The absorption spectra of the lycopene and chlorophylls are complementary, absorbing light efficiently over a substantial part of the solar spectrum. b,c) Reproduced with permission.<sup>[106]</sup> Copyright 2015, Royal Society of Chemistry.

the energy-transfer process in photosynthesis in the context of solid-state semiconductor models, leading to various versions of the “semiconductor model of photosynthesis.” Though

ultimately of limited accuracy, interest in this model prompted researchers to explore the conductivity and photoconductivity of materials such as chlorophyll and hemin (porphyrin from blood). These early studies of thin films of natural porphyrins generated salient conclusions such as the predominance of hole (photo)conductivity and the ability of the molecules to act as both donors and acceptors in solid-state photoinduced charge transfer.<sup>[107–109]</sup> In terms of the bulk DC conductivity properties of dry chlorophyll, conductivity is on the order of  $10^{-10}$  to  $10^{-9} \text{ S cm}^{-1}$  and appears to be dominated by thermally assisted hopping.<sup>[110]</sup> These studies of Inganäs and Lundstrom utilized chlorophyll deposited on top of a lateral interdigitated gold electrode structure, easily allowing access to gases. It was found that oxygen exposure increased conductivity while water vapor actually led to a decrease. The same authors also found that chlorophyll films behaved as photocathodes, with the photocathodic current attributed to the hydrogen evolution reaction. This work was consistent with all the previous findings of chlorophyll being primarily of p-type character. Tang and Albrecht reported in the 1970s a series of experiments studying the conduction of chlorophyll-a in thin-film diode geometries (Figure 6).<sup>[108]</sup> Chlorophyll-a microcrystalline thin films can be conveniently prepared using an electrophoretic deposition method from organic suspensions in solvents such as octane. These thin film diodes gave a photovoltaic effect, albeit with very low photocurrents in the tens of  $\text{nA cm}^{-2}$  range and open-circuit potentials ranging from 200 to 500 mV, and thus power conversion efficiencies around  $10^{-3}\%$ . The photocurrent action spectrum matched the entire optical absorption of chlorophyll-a films. This study also concluded that chlorophyll-a primarily supports p-type conduction. A recent study by Kassi et al. followed up on this work, finding that the Coulombic energy of the photogenerated charge pair is considerably higher than  $kT$ , leading to a greater geminate recombination and resulting in a lower quantum yield,  $\phi$ , of free charge-carrier generation.<sup>[111]</sup> In this respect, chlorophyll is not different than typical organic semiconductors, where the high exciton binding energy necessitates the use of donor–acceptor heterojunctions in order to reach practical levels of photocurrent. The donor–acceptor approach was followed by Duan et al., where it was shown that bacteriochlorophyll derivatives in bulk heterojunction solar cells, with fullerene acceptors; however, power conversion efficiencies remain below 1%.<sup>[112]</sup> Porphyrins have been studied

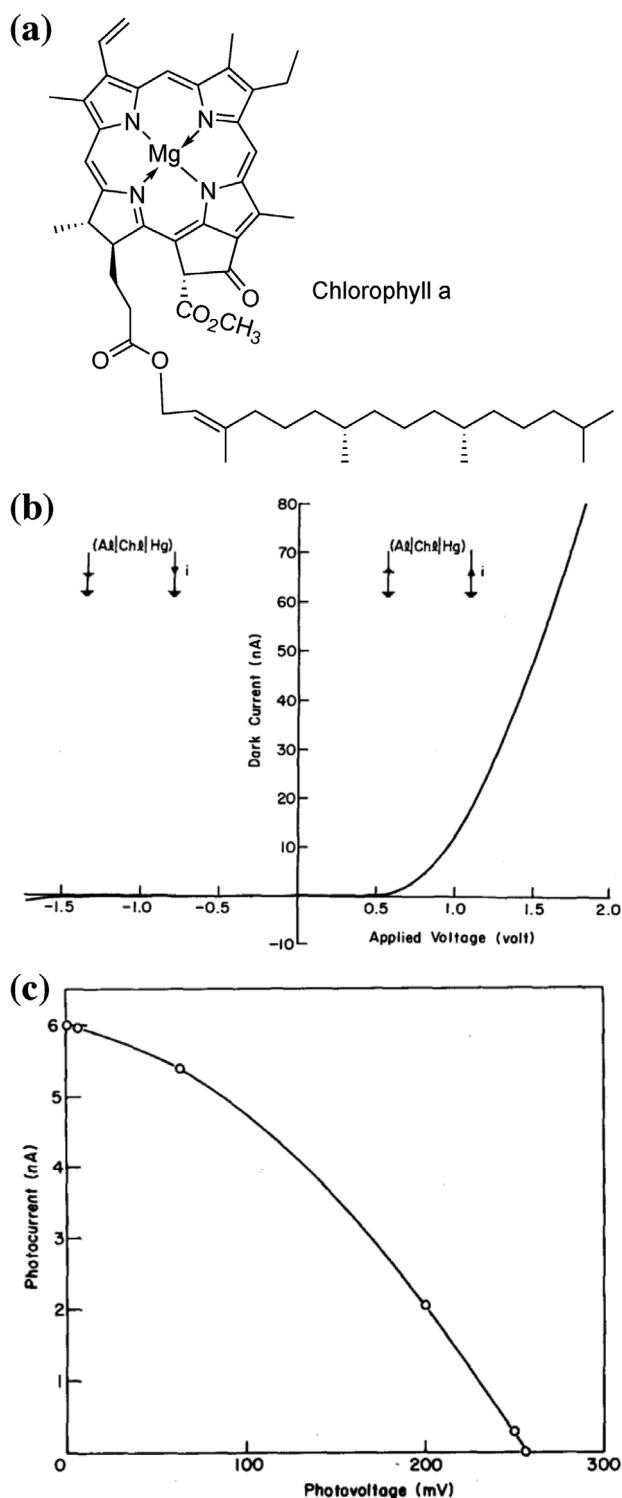


**Figure 6.** Photovoltaic diodes with microcrystalline films of chlorophyll-a. a) The structure of chlorophyll-a. b) Dark and c) illuminated  $I$ - $V$  characteristics. b,c) Reproduced with permission.<sup>[108]</sup> Copyright 1975, American Institute of Physics.

in some detail as sensitizers for various photovoltaic and photoelectrochemical cells; however, these devices do not rely on the bulk conduction of these materials. An important property

of photosynthetic porphyrins is their inherent instability. The evolutionary process that leads to porphyrins as active materials in photosynthesis did not endow them with stability, and instead they are continuously broken down and reconstructed via metabolic processes. As in the case of carotenoids, the stability issue here may be of potential benefit in the context of transient/resorbable<sup>[113]</sup> electronics, where biodegradation is a desired feature.

### 3.2. Large Biological Molecules, Polymers, and Assemblies

In the previous section, we discussed electronic and ionic/protonic conduction across materials that were formed by small molecules, several of which have direct biological significance in (for example) processes such as photosynthesis. In this section, we focus on “larger” biological (or bioinspired) materials, meaning materials that are composed of biological building blocks, for the formation of films, polymers or large assemblies that can conduct charges (electrons or protons) over long distances. In general, these larger building blocks are biopolymeric (a somewhat loose but convenient term that we will henceforth adopt) or bio-macromolecular, and for the purposes of this review we divide them into four main groups: polysaccharides composed of monosaccharides (sugars), proteins composed of amino acids, DNA composed of nucleic acids, and macromolecular indolequinones such as melanins. To this we add a fifth class of “structures”—membranes made up of assemblies of fatty acids, which can be thought of similarly in terms of their electrical properties at least. Among these groups, polysaccharides, melanins, and protein-based materials have been most studied for their macroscopic electrical conduction. As discussed in Section 1, the field of DNA electronics has been restricted to the sub-micrometer length scale regime and so has limited relevance to the discussion herein. It is also important to emphasize that we focus on the “intrinsic conductance,” i.e., the conductance of the material in either the dry or the water-swollen state. This contrasts with many reported measurements where the material is placed in an ion-containing solution (buffer), and the conductance is controlled by the presence of ions rather than the “biopolymer” itself. In the context of these intrinsic properties, we discuss several means to manipulate the conductance via different strategies (Figure 7), namely, 1) chemical modification of the constitute biomolecule—this strategy involves changing the molecular composition of the monomeric units from which the polymer is composed (most often but not necessarily prior to polymerization); 2) blending with a synthetic conducting (electronic or ionic) polymer during or post polymerization or assembly; 3) doping with charge mediating small molecules post polymerization or assembly—we refer to this process as molecular doping, in a direct analogy to the use of “doping” in semiconductors such as silicon in order to modulate free carrier density and thus conductivity; and 4) coating the biopolymer with a conductive polymer—similar to blending, but the conductive polymer is used to coat the biopolymer after its formation. We now address the biopolymeric relevant groups (polysaccharides, proteins, and melanins) with reference to these modification strategies.

### 3.2.1. Polysaccharide-Based Biopolymers

#### Conductance across Natural Polysaccharides:

Polysaccharides are large macromolecules that are composed of long chains of monosaccharides. Polysaccharides are used in nature either for energy storage (such as starch or glycogen) or for structural purposes (such as cellulose, chitin, or pectin). Structural polysaccharides are found mainly in cell walls of plants, algae, bacteria, and fungi, as well as in the exoskeleton (shell) of animals. Usually, but not exclusively, the structural aspect of polysaccharides is evidence in the formation of strong fibers. Structural polysaccharides were one of the first biomolecular polymers to be examined for their electronic conductance properties, mainly due to their large abundance, their important biological role, and the relative ease of making samples. As such, they are still studied as conducting biomolecular polymers. Among the various polysaccharides, the following have been most studied for their electrical conductance: cellulose (a polymer of D-glucose), chitin (a monomer of N-acetylglucoseamine), and particularly chitosan (a deacetylated product of chitin that contains D-glucosamine) (Figure 8). Electrical conductance measurements on polysaccharides started with the pioneering work of Murphy on cellulose in 1960.<sup>[56]</sup> He used condensed paper made of dry cellulose between two tungsten electrodes for measuring electrical conductivity across a very high voltage gradient of  $\approx 50 \text{ kV cm}^{-1}$ . An intrinsic resistivity value of  $10^{18} \Omega \text{ cm}$  was observed at room temperature ( $10^{15} \Omega \text{ cm}$  at  $100^\circ \text{C}$ ), with an activation energy of  $1.33 \text{ eV}$  ( $30.7 \text{ kcal mol}^{-1}$ ), which was attributed to the ionic conduction across the cellulose paper (Figure 9a). Shortly after, very similar conductivity values and activation energy were obtained for the ionic conductivity across cellulose acetate films, the acetate ester of cellulose.<sup>[14]</sup> Hence, cellulose can be considered an insulator in its intrinsic state.

Following these early observations of the apparent lack of conductivity in polysaccharides, there were not any major breakthroughs in this field for around 40 years, until 2003 with the discovery of the ionic conductivity across chitosan films by Creber and co-workers.<sup>[115]</sup> In the latter study, it was found by AC measurements that the intrinsic ionic conductivity of water-swollen chitosan can reach values of  $10^{-4} \text{ S cm}^{-1}$  with different degrees of deacetylation and for different molecular weight chitosans (Figure 9b). In the same study it was also shown that the dry state of chitosan is nearly 5 orders of magnitude less conducting than the water-swollen state of chitosan, but still 9 orders of magnitude more conducting than dry cellulose films. The authors suggested that the ionic conductivity in the swollen state was due to the transport of hydroxide ions ( $\text{OH}^-$ ), which are formed by the protonation of the free amino groups in the chitosan backbone by water molecules ( $\text{chitosan} - \text{NH}_2 + \text{H}_2\text{O} \rightleftharpoons \text{chitosan} - \text{NH}_3^+ + \text{OH}^-$ ).<sup>[115]</sup> However, and with additional hindsight, it is unlikely that this mechanism governs the ionic conductance in chitosan due to the high  $pK_a$  value of water. As discussed below, it is more likely that the

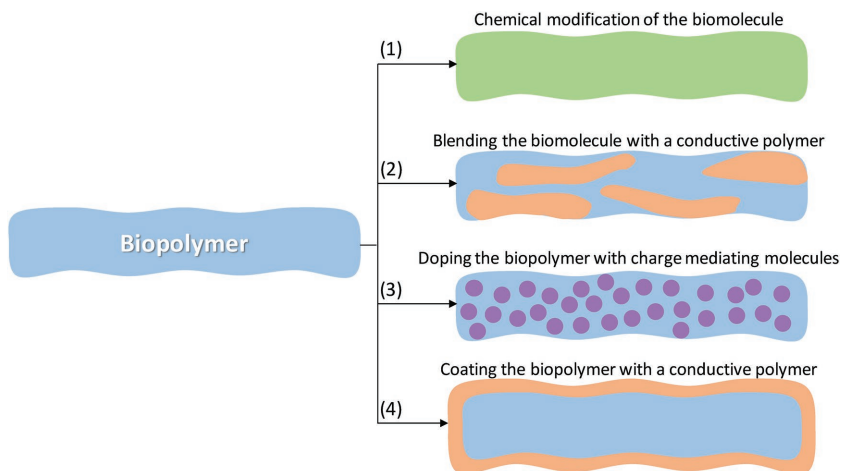


**Figure 7.** Summary of the different modification strategies for changing biopolymer electronic properties: 1) chemical modification of the constituent biomolecules or monomeric units, 2) blending the biomolecule with a conductive, 3) doping the polymer with charge mediating molecules, and 4) coating the biopolymer with a conductive polymer.

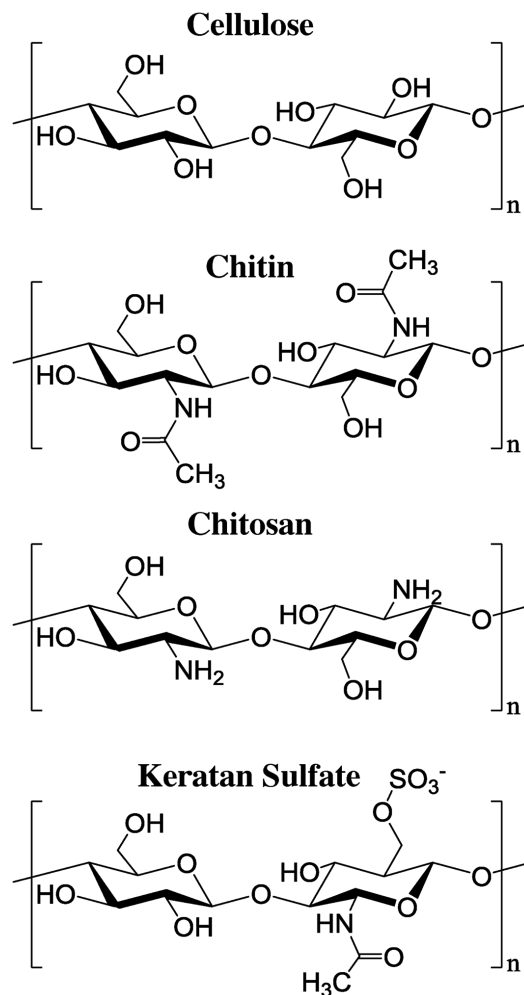


**Figure 8.** Molecular structures of natural polysaccharides. We note the structure of chitosan is the same as for fully acetylated chitin, however also partial acetylation (>50%) of chitin is considered chitosan.

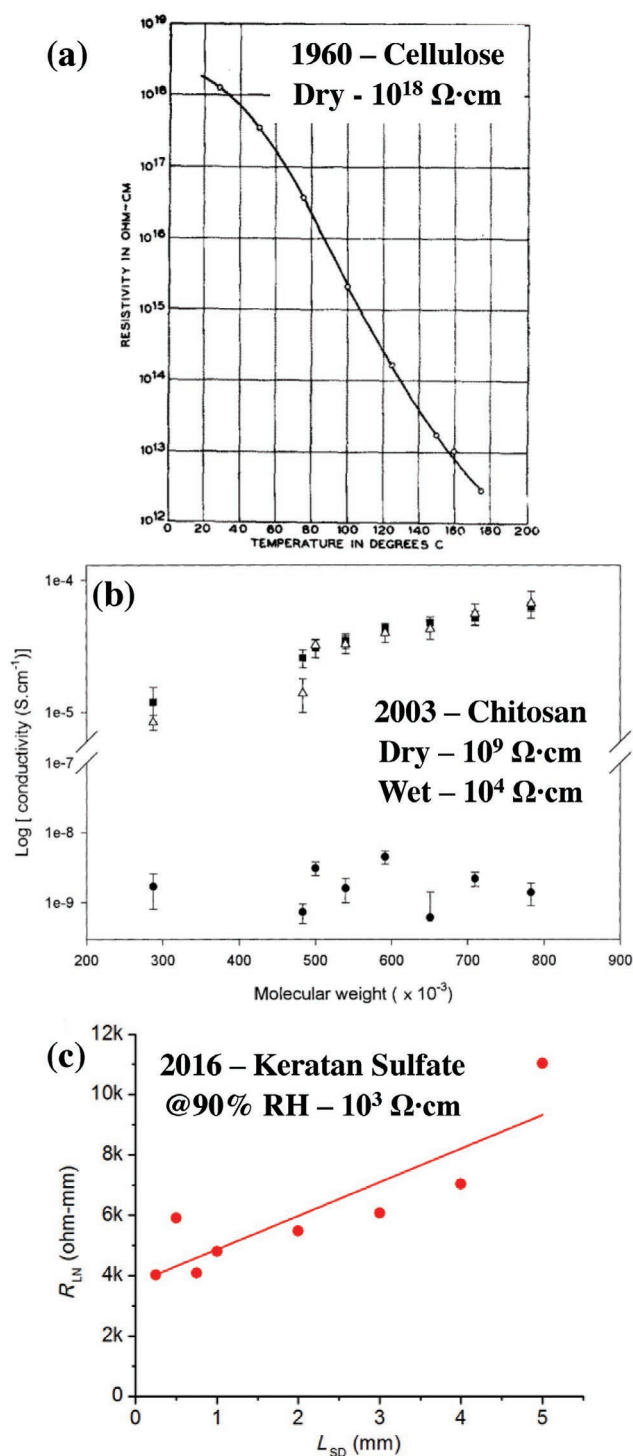


**Figure 9.** Electrical characterization of polysaccharide: a) dry cellulose, b) dry and wet chitosan, and c) wet keratin sulfate. a) Reproduced with permission.<sup>[56]</sup> Copyright 1960, Elsevier. b) Reproduced with permission.<sup>[115]</sup> Copyright 2003, Elsevier. c) Reproduced with permission.<sup>[116]</sup> Copyright 2016, The Authors, published by AAAS.

Grotthuss mechanism is the underlying physics in the proton conduction across chitosan films. Similarly, in a further study comparing chitosan and chitin films, it was found that the

ionic conductivity across chitin films was around  $10^{-6} \text{ S cm}^{-1}$ <sup>[66]</sup> i.e., 2 orders of magnitude lower than chitosan, which emphasizes the role of the amino group of chitosan in the process.

A recent addition to polysaccharide-based ionic conductors was reported by Rolandi and co-workers in the jelly within the *Ampulla of Lorenzini* in sharks and rays.<sup>[116]</sup> They measured the DC conductance across several millimeters of the jelly between two PdH<sub>x</sub> electrodes and observed proton conductivity values of order of  $10^{-3} \text{ S cm}^{-1}$ , which is the highest intrinsic ionic conductivity values measured for a biological polymer—albeit a gel in this case (Figure 9c). They attributed the high ionic conductivity to the presence of keratin sulfate, a sulfonated polysaccharides (Figure 8), where the sulfate groups act to increase the proton conduction in a similar manner to Nafion.

Until now, we have discussed the intrinsic conductivity properties of natural polysaccharides, ranging from the insulating character of cellulose to the partially conductive nature of chitosan and natural sulfated polysaccharides. In all cases, the conductivity was assigned to ionic and especially protonic transport. However, the conductance across polysaccharides can easily be tuned using the different approaches described above. The most common strategies to manipulate the conductance of polysaccharides involve chemical modification of the polysaccharides and the formation of polymer blends with conductive polymers, though strategies involving the addition of doping molecules and the coating of the polysaccharide can also be found in the literature. We will now briefly discuss these two main approaches.

*Conductance across Chemically Modified Polysaccharides:* As can be seen in Figure 8, polysaccharides have functional hydroxyl groups that can be chemically modified. Chitosan is especially attractive in this context as it has an additional free amino group that can be modified. Taken together with its improved ionic conductivity in comparison to cellulose and chitin, chitosan has been extensively studied for its chemical modifications and their contribution to the ionic conductivity across the polymer.<sup>[117]</sup> One of the common modifications to improve the ionic conductivity of chitosan is sulfonation (see Figure 10 for a summary of various chemical modifications),<sup>[118–122]</sup> which can also be used for cross-linking between chitosan chains. Sulfonation modification is an obvious modification choice due to the crucial role of the sulfonic groups in the ionic conductivity in Nafion.<sup>[49]</sup> Other modifications include phosphorylation,<sup>[123,124]</sup> quaternization,<sup>[125,126]</sup> the addition of pyridine,<sup>[127]</sup> maleic acid<sup>[66,128]</sup> and proline.<sup>[128]</sup> The modifications with proline and maleic acid are particularly interesting since the authors<sup>[128]</sup> showed in an FET configuration that the current–voltage gate response could be reversed in a chitosan–maleic acid channel versus chitosan–proline (Figure 11). A reversal in gate polarity is attributed to opposite charge carriers, which the authors explained as having proton conduction across the chitosan–maleic acid sample, and hydroxyl ion conduction across the chitosan–proline sample with mobilities of  $\mu_{\text{H}^+} = 5.3 \times 10^{-3}$  and  $\mu_{\text{OH}^-} = 0.4 \times 10^{-3} \text{ cm}^2 \text{ V}^{-1} \text{ s}^{-1}$  for protons and hydroxyls, respectively.<sup>[128]</sup> The authors explains the mechanism of conduction using the Grotthuss mechanism and its modification to encounter also hydroxyls mobility. Overall, most of the chemical modifications of chitosan showed an increase in the conductivity values from  $10^{-5}$  to  $10^{-4} \text{ S cm}^{-1}$

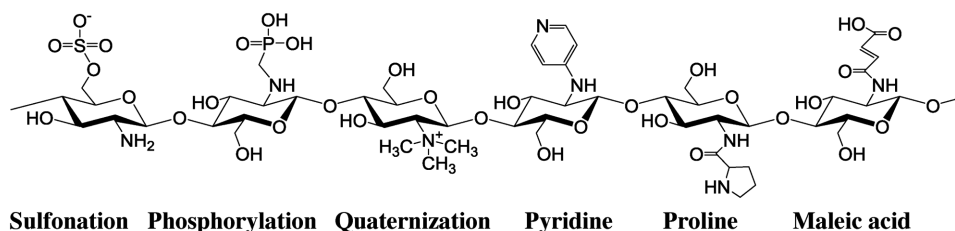


**Figure 10.** Several examples for the chemical modifications of chitosan.

for swollen chitosan films, and up to impressive values in the order of  $10^{-2} \text{ S cm}^{-1}$ . The lower resistance across the chemically modified chitosan polymers is due to three main reasons: 1) the additional groups usually provide sites that can be protonated during a Grotthus type proton hopping mechanism (further discussion in the mechanism section); 2) the addition of hydrophilic moieties increases water absorbance into the chitosan polymer, which in turn increase the ionic conductivity across the material by introducing water channels; and 3) cross-linking by chemical modification reduces the crystallinity of the chitosan films, thus increasing the fraction of amorphous phase which is the proton transport medium.<sup>[129,130]</sup>

*Conductance across Blends of Polysaccharides with Other Polymers:* Unlike chemical modification, the formation of multipolymer blends is less defined, but it is a very simple methodology that can result in a new material having the desirable properties of the two blended systems. As in the previous approach, chitosan has been extensively used, in either its natural or chemically modified state, for blending with other polymers for improved ionic conduction or for improved mechanical properties. The blending can be achieved by simply dissolving the two polymers in each another, such as in the formation of chitosan–poly(vinyl alcohol) blends,<sup>[124,131–133]</sup> or by driving electrostatic interactions (ionic cross-linking) between the cationic state of chitosan and an anionic polymer, such as in the formation of chitosan–poly(acrylic acid).<sup>[134,135]</sup> Chitosan has also used in blends with Nafion, and to coat Nafion for achieving better ionic conduction or to introduce biofunctionalization.<sup>[136–139]</sup> In an additional interesting study, small hormone biomolecules similar to the ones we discussed in the previous section were also blended into chitosan for

improved ionic conductivity<sup>[140]</sup>—although this in reality is the formation of a composite material by molecularly doping. Outside the scope of this review, the formation of chitosan-based composite materials has been studied extensively mainly via the incorporation of inorganic molecules or structures, and further discussion and examples can be found in alternative review papers.<sup>[117,141]</sup>

In a similar manner to the blending of ionic systems, electron conducting polymers can also be blended into polysaccharides for the formation of electron conducting mixed polymers. In this approach, the polysaccharide can be considered merely as a template since it does not contribute to the electronic conductivity of the mixed polymer. As such, cellulose is a good candidate due to its natural abundance. Indeed, several studies have investigated blends of cellulose with electron conductive molecules/polymers, such as carbon nanotubes,<sup>[142,143]</sup> graphene,<sup>[144]</sup> polyaniline,<sup>[145,146]</sup> and polypyrrole<sup>[147–149]</sup> motivated by the development of conductive paper for “green electronics.” Chitosan and chitin have also been used as templates for the formation of electron conducting polymers upon blending with polyaniline,<sup>[150–152]</sup> carbon nanotubes,<sup>[153]</sup> or graphene.<sup>[154]</sup> The strategy of using carbon nanotubes and graphene for enhanced conductance across the biopolymer can be considered as an intermediate between strategies (2) and (3) in Figure 7, since they are not organic polymers, but have considerably larger molecular weights than molecular dopants. Recent advances in the field demonstrate the use of polysaccharide-based nanofibers for the formation of transparent polymers on which a conducting layer can be deposited for various electronic applications and further discussion on this matter can be found in the application section.<sup>[155–158]</sup>

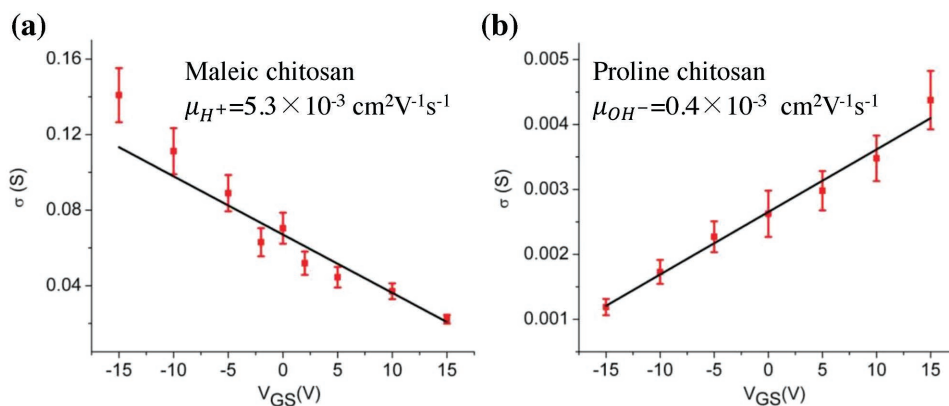


**Figure 11.** a,b) Electrical response of an FET with maleic acid (a) and proline-modified chitosans (b). Reproduced with permission.<sup>[128]</sup> Copyright 2013, Springer Nature.

### 3.2.2. Peptide- and Protein-Based Structures and Biopolymers

Proteins are macromolecules that are formed by the folding of long amino acid chains. Peptides are merely small proteins having less than 40–50 amino acids in their chains. Proteins and peptides are the outcome of the genetic code, and are synthesized in nature within ribosome complexes during the translation process from mRNA. Most cellular activities are controlled by proteins, such as enzymatic activity, signal transduction, transmembrane channel activity, cellular receptors, etc. An additional class of proteins and peptides include the ones that can form very long fibrillar structures by a self-assembly process. Protein-based structures can be intracellular, such as the protein fibers that form the cytoskeleton (as microtubules and actin filaments) or extracellular, such as the proteins that form the extracellular matrix (collagen and elastin) or indeed those present outside of the body (such as keratin within the hair, wool, and skin or fibroin proteins that form silk). They are a diverse, complex and critical family of biopolymers that we have barely touched in terms of technological potential.

**Early Observations:** As discussed in the introduction, the relevant solid-state electrical study of protein-based materials started in the 1960s with work on films that were formed by globular proteins (hemoglobin and cytochrome c) or fibrous proteins (collagen, silk, and wool).<sup>[14,32,55]</sup> However, it is hard to consider some of these experiments as “electrical measurements on biopolymers” since they involved studies of various thickness monolayers formed by gas evaporation of the biological molecule by the Brunauer–Emmett–Teller (BET) method. Thus, the main conclusions we can draw from these early experiments concerns the different role of water in supporting long-range ionic conductivity between the protein-based structures of silk and wool versus that in conduction across cellulose.<sup>[55]</sup> In 1976, Murphy conducted the first temperature-dependence DC conductance measurement across wool (keratin protein) in the dry state.<sup>[159]</sup> A measurable conductance was only observed at elevated temperatures of above 140 °C, where the conductivity across the film was of order of  $10^{-12}$  S cm<sup>-1</sup>. By extrapolating to room temperature using the calculated activation energy a value of  $10^{-17}$  S cm<sup>-1</sup> was inferred, i.e., characteristic of an insulating material but nevertheless the authors ascribed the elevated conductivity at high temperatures to ionic conduction across the wool.

The role of water content on the ionic conductance across protein biopolymers was reported by Bardelmeyer et al. in 1973 in their work with collagen (in a form of a tendon).<sup>[160,161]</sup> It was demonstrated that the room temperature conductivity across collagen could be increased from  $\approx 10^{-11}$  S cm<sup>-1</sup> at a water content of 8.5% to  $\approx 10^{-3}$  S cm<sup>-1</sup> at saturation. It was further observed that the activation energy of the conductance decreased from a value of 1.15 eV to 0.31 eV under the same conditions, with a linear change as a function of water content with two different slopes before and after the value of 50% water content. This change in slope was attributed to proton conduction at lower water contents, and larger ion conduction at higher water contents. In further discussion on the matter by the same authors,<sup>[161]</sup> they addressed the issue of the different contributions to the conductance of bound and loose water molecules within the structure—a concept that is highly relevant to

more modern studies (not just in proteins), and often ignored. Protein-bound water molecules have fundamentally different properties to loosely bound “matrix” water molecules. Protein-bound water molecules can be considered as part of the protein structure, they are tightly bound, they cannot be released in vacuum and they do not freeze. Tightly bound water molecules have been shown to have a crucial role in mediating the transport of protons across proteins in biological system,<sup>[162,163]</sup> and further discussion on the role of water molecules in conduction is given in the mechanism section. Despite this early progress, there were not any major breakthroughs in the field of electrical conductivity across peptide- or protein-based biopolymers for several decades thereafter, which is likely due to the insulating nature of relatively “dry” protein-based biopolymers. However, as we will detail below, this situation has recently changed.

**Silk-Based Biopolymers:** Work on modified protein-based biopolymers started only in the recent decade, and one of the most studied protein-based biopolymers in this context is silk. Silk is made of the fibroin protein, which is rich in poly(Ala-Gly) repeat units, and forms  $\beta$ -sheet structures (Figure 12a).<sup>[164]</sup> The reasons for the abundance of studies on silk are mainly due to its attractive mechanical properties (silk fibers are very strong) and its importance in the textile industry—there is a ready supply of natural silks. The common strategy for increasing the conductivity across silk threads is by coating them with organic conducting polymer such as polyethylenedioxythiophene polystyrene (PEDOT:PSS) (see for example Figure 12b for an image of a coated silk thread),<sup>[165–167]</sup> polypyrrole,<sup>[166,168,169]</sup> and polyaniline,<sup>[166]</sup> or coating with graphene/carbon nanotubes.<sup>[170–172]</sup> These coatings have resulted in impressive measured conductivities of up to  $10^{-1}$  S cm<sup>-1</sup> for the conductive organic polymer coatings<sup>[165,166]</sup> and  $10$  S cm<sup>-1</sup> for the graphene coatings.<sup>[171]</sup> All of these examples cited explore the formation of electronically conducting silk-based material, and we could find only one example for the formation of ionic conducting silk-based polymer by mixing silk in a solution of an ionic liquid and gelatin.<sup>[173]</sup>

In addition to the use of natural silk meshes, which are already considered biopolymers with macroscopic dimensions, several techniques have been developed to create highly packed silk fibers of controllable fiber diameter, with the most common being electrospinning.<sup>[174]</sup> In electrospinning, a dissolved polymer is electroinjected from a conductive needle onto a conductive substrate using high kV voltages between the needle and substrate. Electrospun silk mats (much like silk meshes) are not conductive ( $<10^{-14}$  S cm<sup>-1</sup>).<sup>[175]</sup> However, the electrical conductivity can be increased by coating/adsorbing/doping with carbon nanotubes (see Figure 12c,d for an image and electrical characterization of the modified silk mat),<sup>[175]</sup> blending with graphene solutions<sup>[176]</sup> or coating with polypyrrole,<sup>[177]</sup> up to a conductivity of  $\approx 10^{-4}$  S cm<sup>-1</sup>.

**Peptide-Based and Especially Amyloid-Based Biopolymers:** One of the most-studied protein fibrils in biology are self-assembled amyloid-like fibrils. Amyloid fibrils are part of the etiology of amyloid-related diseases (such as Alzheimer’s, Parkinson’s, and many more), where soluble small proteins (usually peptides) self-assemble into insoluble long amyloid fibers. The mechanism of formation and the role of the fibrils in the progression of neurodegenerative diseases is a massive area of research

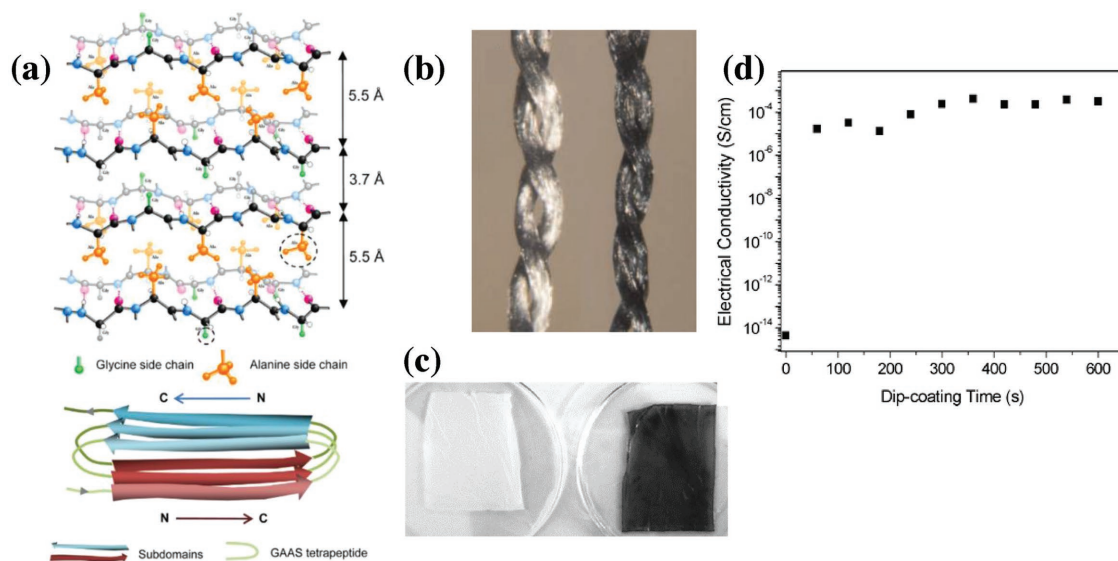


**Figure 12.** a) A molecular structure and a model of silk fibers made of fibroin proteins. b,c) Images of silk threads (b) and silk electrospun mats (c) before (left images) and after modification (coating, absorbing, or doping) (right images) with PEDOT:PSS and carbon nanotubes for (a) and (b), respectively. (d) shows the immediate increase in conductivity of the silk mats in (c) upon coating with carbon nanotubes. a,b) Reproduced with permission.<sup>[164]</sup> Copyright 2015, Elsevier. c) Reproduced under the terms of the CC BY License.<sup>[165]</sup> Copyright 2012, The Authors, published by Public Library of Science. d) Reproduced with permission.<sup>[175]</sup> Copyright 2007, Springer.

in the medical and biological sciences. In this review, we just focus on their structural nature. In this regard, the most common feature of all natural amyloid fibrils is their cross-beta structure (Figure 13a),<sup>[178,179]</sup> which forms a narrow fibril with a thickness of 2–6 nm that can span several micrometers in length. Amyloid fibrils also have a tendency to aggregate and form bundles or networks and like other protein-based structures they are not conductive in their dry state.<sup>[180]</sup> Similar to the silk-based biopolymers, the first strategy to use amyloid fibrils for the formation of conductive biopolymers was to coat them with conductive organic polymers such as PEDOT<sup>[181,182]</sup> or polyaniline (Figure 13b).<sup>[180]</sup>

An additional and rather novel strategy to form conductive wires from amyloid proteins has been recently introduced by Altamura et al.,<sup>[183]</sup> with the genetic expression of a chimeric protein that was composed of a prion domain (an amyloid fibril forming domain) and rubredoxin (an iron containing redox protein). In this technique, the prion domain induces the

creation of the amyloid fiber, which in turn forces the formation of an ordered 1D assembly of the redox protein (Figure 13c). Following expression, thin (5 nm) amyloid fibrils could be observed, which aggregated to form a viscous gel. The authors then dried the gel by drop-casting to form a film, which they showed to have improved electrical properties (electrochemical redox activity and low resistance). The results were explained using a mechanism that involves multiple redox events (hopping) across closely packed redox centers ( $\approx 1$  nm between redox centers) of the rubredoxin protein.

One of the driving forces for the fibrillization of amyloid proteins is the presence of specific amino acid sequences within the amyloid protein termed the “core recognition motif.” For instance, the (AA)KLVFF sequence within the  $\beta$ -amyloid protein is strongly associated with the Alzheimer’s disease.<sup>[184,185]</sup> Short peptides with the sequence of the core recognition motif (or similar sequences) can both inhibit the fibrillization process, as well as forming similar amyloid-like structures by

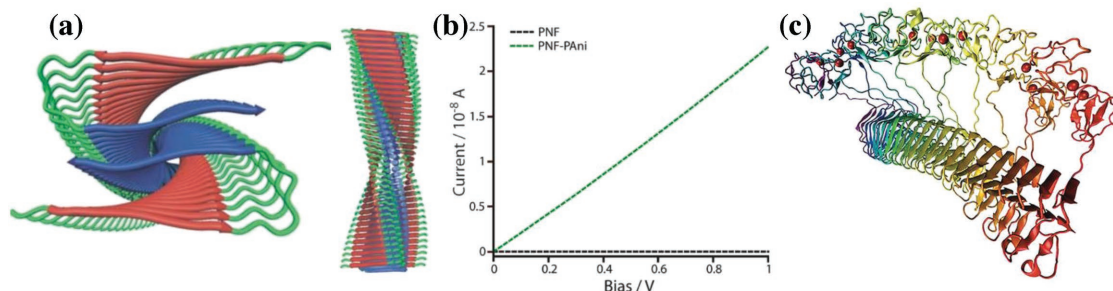


**Figure 13.** a) Top and side views along the z-axis of a model for the cross-beta structure of amyloid fibers. Reproduced with permission.<sup>[179]</sup> 2006, Cambridge University Press. b) An example to the increase in conductance upon coating of amyloid fibrils with polyaniline. Reproduced with permission.<sup>[180]</sup> American Chemical Society. c) A model for an amyloid fibril that was formed by a chimeric protein of a prion domain and rubredoxin. Reproduced with permission.<sup>[183]</sup> Copyright 2017, Springer Nature.

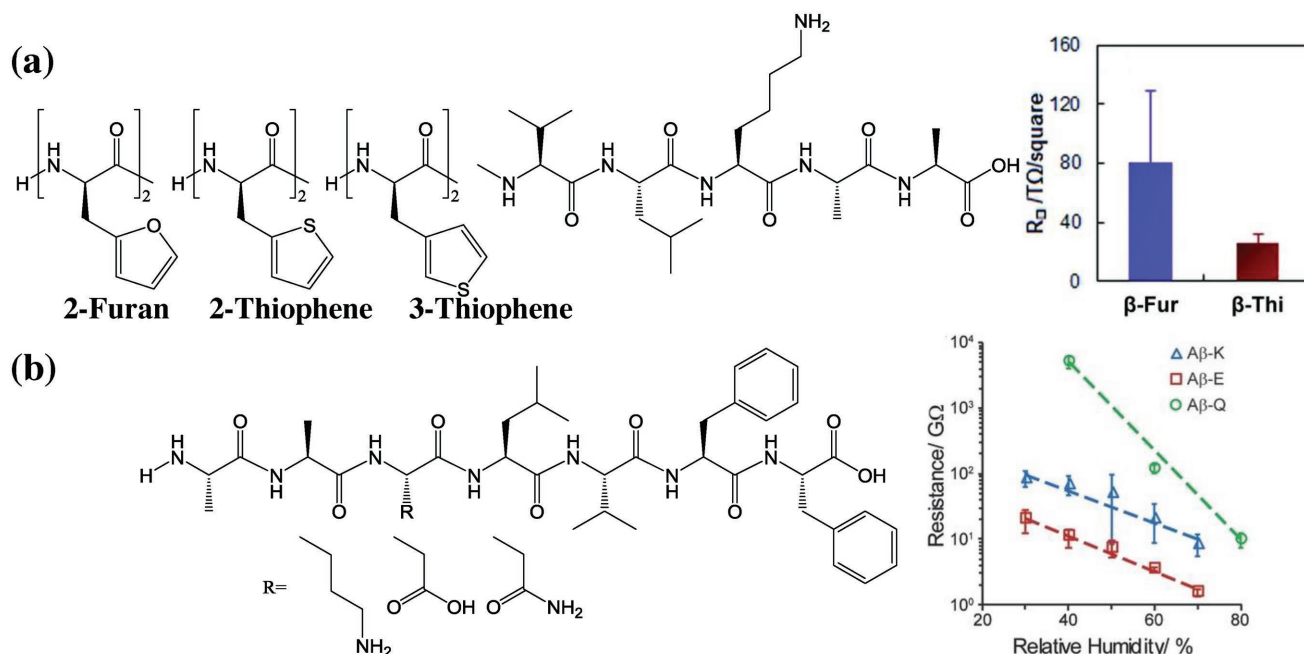


**Figure 14.**  $\beta$ -Amyloid core-recognition-motif-based peptide: a) (di-2-furan-/di-2-thiophene-/3-thiophene-)VLKAA, and the resistance of the films made by the di-2-furan-/di-2-thiophene modifications. Reproduced with permission.<sup>[189]</sup> Copyright 2014, Wiley-VCH. b) AA(K/E/Q)LVFF, and the resistance as a function of relative humidity of the different amino acids substitutions. Reproduced with permission.<sup>[190]</sup> Copyright 2017, Wiley-VCH.

themselves.<sup>[186]</sup> In recent years, Ashkenasy and co-workers have used these short peptides as well as other fibril-forming short peptides to increase the conduction across amyloid-like fibrils.<sup>[187–191]</sup> The main advantage of using short peptide sequences is the relative ease of chemical modifications in terms of amino acids and sequence changes. The authors have used several peptide models and their modifications for investigating long (several micrometers) conduction across a peptide fibril network that was deposited (drop-casted) on top of metal electrodes. For example, peptide models have been investigated based on the core recognition motif of the  $\beta$ -amyloid protein (AAKLVFF), where the Phe (F) residues have been replaced by modified amino acids with a thiophene or a furan group (Figure 14a),<sup>[187–189]</sup> or the replacement of the Lys residue (K) with Glu (E) or Gln (Q) (Figure 14b).<sup>[190]</sup> It was found in this system that the fibrils formed by the modified peptide sequence had higher conductances than fibrils formed by the original peptide motif sequence. This was attributed to changes in the morphology (reorganization) of the fibril, as well as to the presence of the aromatic heterocycles. It was further observed by applying both AC and DC bias and changing the relative humidity, that the thiophene-containing peptide fibrils exhibited both electron and proton conductivity.<sup>[187]</sup> In a similar type of conduction measurements, it was also observed that substituting the Lys residue with Glu resulted in more than an order of magnitude increase in conductance across the fibrils networks, while the Gln substitution resulted in a significant decrease in conductance (Figure 14b).<sup>[190]</sup>

Another group of fibril-forming peptides that belong to the short peptide family but bear no resemblance to amyloid proteins/peptides in terms of the amino acid sequence are termed amyloid-like structures. Several amyloid-like structures

which can self-assemble from diverse peptide building blocks have been studied for their electrical conduction properties (Figure 15).<sup>[191–194]</sup> Ashkenasy and co-workers<sup>[191]</sup> have shown that both electrostatic and aromatic interactions can induce the fibrillization of (FKFE)<sub>2</sub> peptides to thin (3–5 nm) fibrils in water. They further showed that the fibrils are not conductive, but can gain conductivity by replacing one of the phenylalanines with a naphthalene diimide (Figure 15a) modified amino acid, and especially when the fibril is formed in water, i.e., when the amine and carboxylic groups are charged positively and negatively, respectively. Ulijn and co-workers<sup>[192]</sup> have used an Fmoc-LLL protected peptide (Figure 15b) to form fibrils of 13–16 nm thickness that can create a network. They measured low conductances of the network in vacuum, which they attributed to electron transport across the Fmoc moiety. Upon transferring the fibrils to air, they observed more than 3 orders of magnitude increase in conductance, which they attributed to adsorbed moisture in the network. Nakayama and co-workers<sup>[193]</sup> have used the FPRFAGFP peptide (Figure 15c) to form very narrow ( $\approx$ 1 nm) peptide fibrils. They found that the formed fibrils were 3 orders of magnitude more conductive in vacuum compared to films of other proteins. They attributed their findings to electron transport due to the stacking of the phenylalanines aromatic side chain in the fibril structure. The last example in this category is the work of del Mercato et al.<sup>[194]</sup> who used the VGGLG peptide (Figure 15d) to form relatively thick amyloid-like fibrils with diameters of more than 20 nm. Their observation of electrical conduction across the fibril network is interesting as it is the only example so far without any conjugated aromatic moieties in the peptide sequence. They likewise attributed their observations to the formation of water containing hydrogen bonded networks between the peptides in



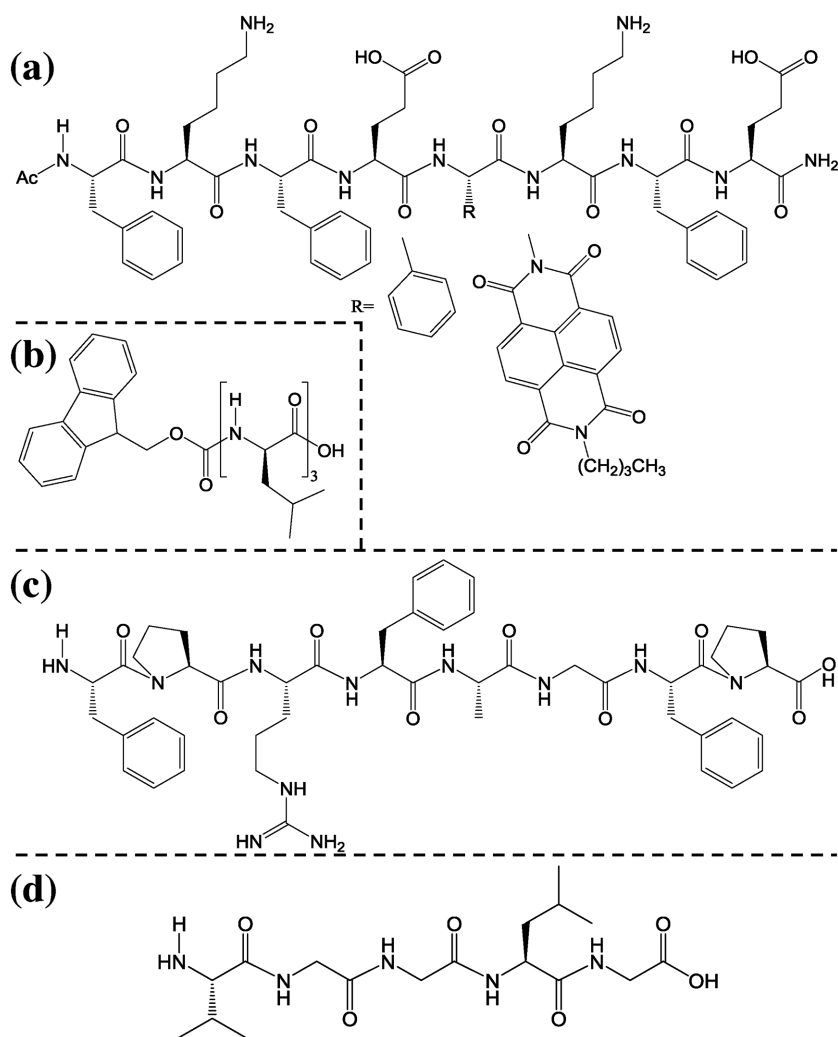


**Figure 15.** Peptide models for the formation of amyloid-like structures. a) (FKFE)<sub>2</sub> sequence with a naphthalene diimide modification.<sup>[191]</sup> b) Fmoc-LLL.<sup>[192]</sup> c) FPRFAGFP.<sup>[193]</sup> d) VGGLG.<sup>[194]</sup>

the final structure, and although the authors did not discuss the mechanism it is most likely that the Grotthuss mechanism was involved in their system.

Alternative approach of using peptides for the formation of electron conducting materials was developed by the group of Tovar who designed a unique form of peptide amphiphiles, where short peptide sequences (3–5 amino acids) were attached to the two ends of an oligo-phenylenevinylene or an oligothiophene segment (Figure 16a).<sup>[195–199]</sup> In this configuration, the peptides direct the self-assembly of the molecule to a 1D fibril composed of  $\beta$ -sheet structure, and resulting in the stacking of the oligo-phenylenevinylene or oligothiophene units to form a  $\pi$ -conjugated structure (Figure 16b). They showed that the presence of the  $\pi$ -conjugation could result in an efficient photoinduced energy transfer,<sup>[196,198]</sup> photoinduced electron transfer,<sup>[199]</sup> as well as electronic semiconducting properties.<sup>[195,197]</sup> The latter type of experiments were performed in an organic field effect transistor configuration (Figure 16c). Interestingly, although the  $\pi$ -conjugation is responsible for the semiconductivity of the structures, the authors observed 3 orders of magnitude difference in

the electron (hole) mobility for different peptide sequences, ranging from  $\approx 5 \times 10^{-5}$  to  $\approx 2 \times 10^{-2} \text{ cm}^2 \text{ V}^{-1} \text{ S}^{-1}$  for peptide sequences of Glu-Val-Val and Asp-Gly-Gly, respectively.<sup>[195]</sup> They explained their finding by the bulkiness of the amino acids situated next to the oligothiophene, where bulkier amino acid (Val) will disrupt the  $\pi$ -conjugation compared to a less bulky amino acid (Gly). They further prove that the amino acids themselves have no role in the electron conductance by using controls without the oligothiophene. In the same study, they also showed that the peptide-based semiconductor could even serve as the gate electrode itself (Figure 16d), and they verified it using a common pentacene film.

In a short summary, peptide-based systems that can form amyloid-like thin fibrils are highly attractive models as they provide an unlimited playground for chemical modifications in terms of amino acid sequence and the use of modified amino acids. However, the main disadvantage is the difficulty in forming a uniform polymer/layer from the self-assembled fibrils, in contrast to biopolymers from polysaccharides, silk or other proteins (as will be discussed below). The inability to form a 3D biopolymer macroscopic structure makes it impossible to discuss the conductivity values of amyloid-like structures and to compare them to other biopolymeric systems.

**Nonfibril Proteins:** The last group of materials that will be discussed in this subsection consists of proteins that do not form fibrils in their natural environment, but can form biopolymers/films under some conditions and that possess respectable conducting properties. Though conductance measurements across films of nonfibril proteins began more than 40 years ago,<sup>[200]</sup> only much recently (in the last 4 years), there is a significant progress. The first protein in this nonfibrillar group worthy of mention is reflectin, which is a cephalopod structural protein that aggregate to form platelets in the skin of the cephalopod. Gorodetsky and co-workers have used this protein in several studies for the formation of a proton conducting biofilm,<sup>[201–204]</sup> mainly due to the relatively high percentage of charged amino acid within it. In their first study from 2014,<sup>[202]</sup> they measured the conductivity across a drop-casted film of reflectin (at room temperature and a high relative humidity of 90%) to be on the order of  $10^{-4} \text{ S cm}^{-1}$ , with an activation energy of 0.22 eV (Figure 17a). They attributed the measured conductivity to proton transport via the Grotthuss mechanism based upon a kinetic isotope analysis (Figure 17b) and the strong humidity dependence (Figure 17c). It was postulated that the high prevalence of charged amino acids, and especially oxo-amino-acids (Asp and Glu) in the reflectin protein are critical factors in delivering proton transport. In order to examine this hypothesis the authors used a

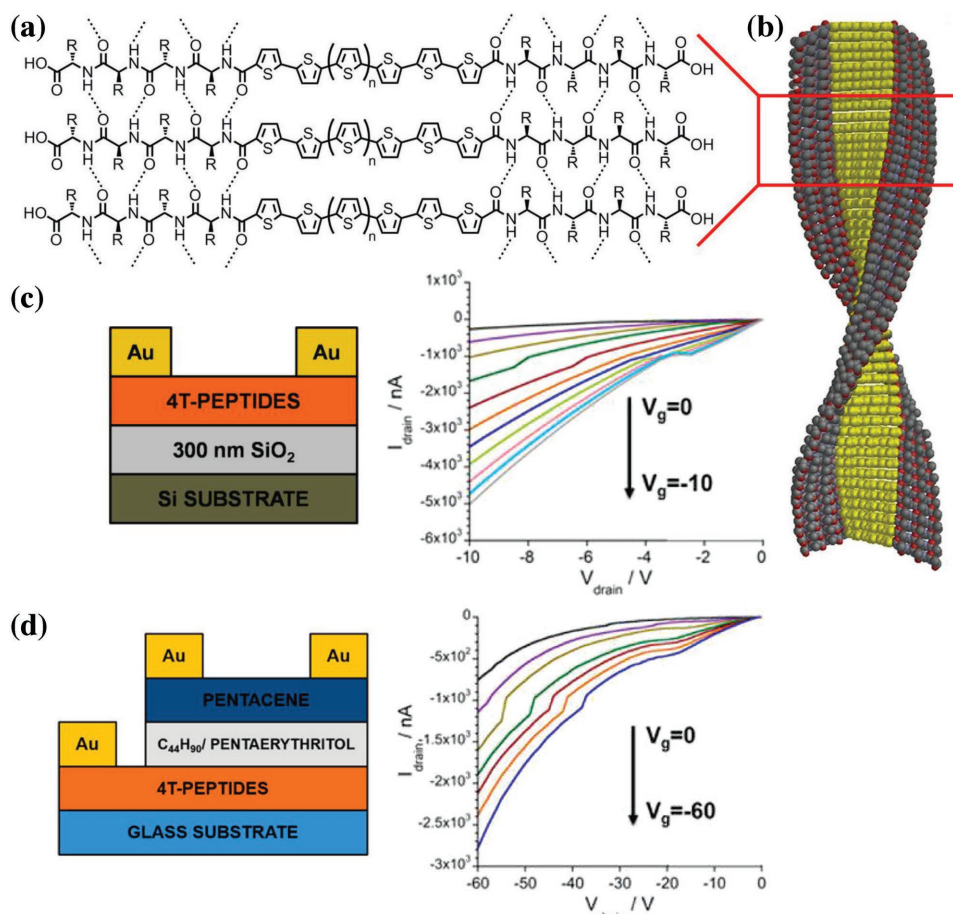


**Figure 16.** Conductive peptide amphiphiles. a) Molecular structure of the structures. The scheme shows oligothiophene, though oligo-phenylenevinylene can be used as well. b) The organization of the molecules to a 1D fibril with a  $\beta$ -sheet motif. a,b) Reproduced with permission.<sup>[195]</sup> Copyright 2015, American Chemical Society. c) Schematic of the use of the peptides in transistor configuration along with an  $I$ - $V$  output curves as function of gate voltage. d) Schematic of the use of the peptides as the gate electrode of the transistor along with an  $I$ - $V$  output curves as function of gate voltage. c,d) Reproduced with permission.<sup>[197]</sup> Copyright 2012, American Chemical Society.

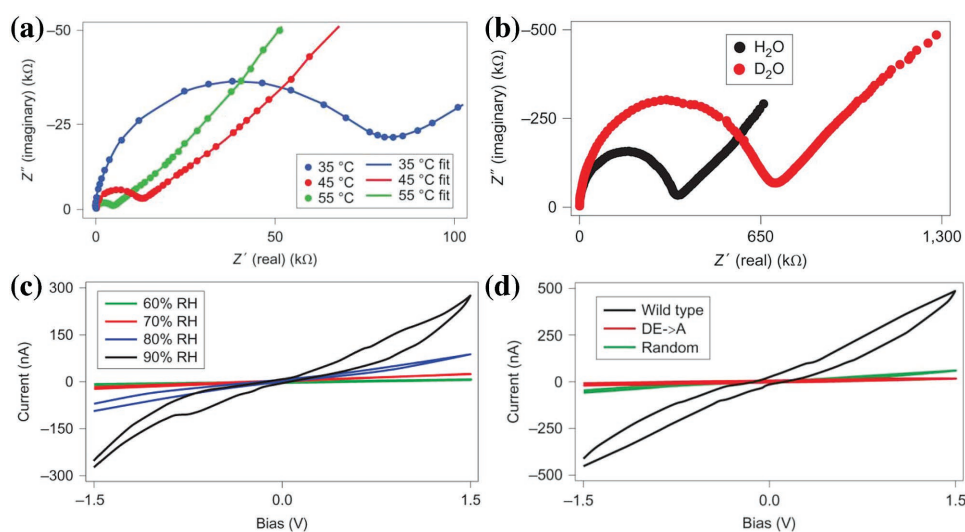


**Figure 17.** Electrical characterization of the reflectin protein films. a) Temperature dependence. b) Kinetic isotope effect. c) Relative humidity dependence. d) Change in conductance upon mutating the Asp and Glu to Ala or scrambling the sequence. Reproduced with permission.<sup>[202]</sup> Copyright 2014, Springer Nature.

genetically modified protein where all the Asp and Glu acids in the protein were replaced with Ala residues, and, indeed, they observed an order of magnitude decrease in conductance across the mutated reflectin films compared to the wild-type (Figure 17d). Using an FET configuration, they further extracted a proton mobility of  $\mu_{\text{H}^+} = 7.3 \times 10^{-3} \text{ cm}^2 \text{ V}^{-1} \text{ s}^{-1}$  and charge (proton) carrier concentration of  $n_{\text{H}^+} = 10.6 \times 10^{16} \text{ cm}^{-3}$ .

A second protein family that has been examined for its conducting properties is the globular protein family of albumins. A common subgroup of this family is serum albumin, which is the most abundant protein in vertebrate blood. Another protein family member is ovalbumin, which comprises more than 50% of egg white proteins, and accordingly egg white is termed albumen. In 2016, Wu et al.<sup>[205]</sup> used albumen for the formation of films on an indium tin oxide (ITO) electrode by spin coating, and they measured both the in-plane (across the surface of the film) and out-of-plane (across the thickness of the film) conductance of the albumen film attributing both to proton transport. They found an out-of-plane conductivity of order  $10^{-4} \text{ S cm}^{-1}$ . For the in-plane electrical measurements an unconventional transistor configuration was used with in-plane gating electrodes—although no conductivity values were actually reported. In another study of the same year (2016), Amdursky et al.<sup>[206]</sup> used bovine serum albumin for the formation of freestanding large protein mats (Figure 18a), and they measured the conductance across the water-swollen mats (in-plane) to be in the order of  $10^{-5} \text{ S cm}^{-1}$ . They attributed the measured conductance to proton transport, and by invoking a photoinduced proton transfer hypothesis, they speculated that charged amino acids of the protein had a role in the proton conduction mechanism. In their follow up study,<sup>[207]</sup> Amdursky et al. used one of the well-known biological properties of serum albumin to tightly bind a variety of small molecules, in order to

molecularly dope the serum albumin mats with hemin. Hemin (an iron containing porphyrin) is commonly used in biology as an electron mediator, and apparently, it is the mediator of long-range extracellular electron transport across the bacterial nanowire.<sup>[208,209]</sup> The authors showed that hemin can bind strongly to the serum albumin mats (Figure 18a) with doping levels comparable to highly doped silicon, and that the hemin molecules do not leach out of the mats when placed in an aqueous solution. Following doping, the conductivity across the mats increased to a value of  $10^{-3} \text{ S cm}^{-1}$  (Figure 18b). They attributed this large increase (nearly 2 orders of magnitude) in conductance to the addition of hemin-mediated electron conduction via the hopping mechanism. Accordingly, the doped serum albumin mats could be considered as a mixed (electron and proton) conductors.

### 3.2.3. Melanin- and Polyindolequinone-Based Biopolymers

As described in the Introduction, the biopolymer melanin was one of the first to be studied in detail in relation to its macroscopic electrical conductance.<sup>[26,32,41]</sup> There are several reasons why melanin (and in particular the brown-black pigment eumelanin) became an early model system: notably the ubiquity of melanins in the biosphere; the availability of multiple natural sources (for example sepia melanin); and the relative ease of making a synthetic model from dihydroxyphenylalanine (DOPA) or tyrosine usually purified in powder form then pressed into pellets for somewhat repeatable solid-state measurements. Indeed, melanins are different from the other biopolymers discussed above in that they have *only* been studied in relation to macroscopic electrical properties with no reported measurements on (for example) isolated macromolecules. The explanation for this lies in a fundamental underlying characteristic of all melanins—their intrinsic disorder at virtually all levels of structural organization. In the mid-2000s, Meredith and co-workers developed the so-called “structural disorder model” to explain several key physical properties in melanin—notably the broad band absorbance.<sup>[210]</sup> It is now an accepted paradigm that no two melanin molecules are the same and so single-chain-level electrical studies have questionable relevance. Melanin properties are defined by “emergent collectivism.”

*Melanin Switches and Memory Device:* The field of melanin electronics was initiated by the work of McGinness and Proctor in the early 1970s. In two landmark papers,<sup>[15,16]</sup> they observed reversible switching between two resistive states in a millimeter-scale melanin sample sandwiched between two gold-leaf electrodes. McGinness and Proctor claimed this observation was clear evidence of amorphous semiconductivity (mechanistically discussed in Section 2)—a controversial concept at the time (and indeed now). However, as discussed below, we now understand this electrical switching behavior in terms of protonic currents and space charge effects at non-Ohmic and electrochemically active electrodes. That said, there are examples of more recent reports claiming resistive switching in melanin: for example Di Mauro et al.<sup>[211]</sup> and Ambrico et al.<sup>[212]</sup> The former relying on capacitive ion drift with a strong hydration dependence, but the latter invoking a semiconductor-like argument with trapping and detrapping of electronic carriers.

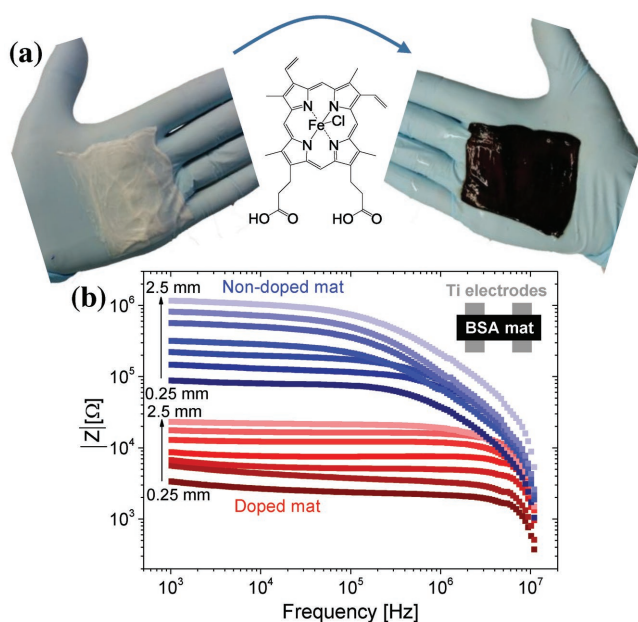


**Figure 18.** a) Doping a large (centimeter scale) mat of serum albumin with hemin molecules. b) The change in resistance upon doping the mat. Adapted under the terms of the CC BY License.<sup>[207]</sup> Copyright 2017, The Authors, published by Wiley-VCH.

Melanins have a considerable capacity for absorbing and binding atmospheric moisture, and this property and the resultant changes to dielectric constant, polarizability, and local equilibrium dynamics of ionizable groups have a profound effect on electrical conductance as discussed below. Indeed, there have been reports of very large dielectric constants,<sup>[41]</sup> ferroelectric behavior,<sup>[213]</sup> and most notably high capacity melanin electrodes for biocompatible energy-storage devices.<sup>[214]</sup> The latter study reported sodium ion loaded melanin anodes exhibiting specific capacities of  $\approx 30 \text{ mAh g}^{-1}$ , and full cells composed of natural melanin anodes and  $\text{MnO}_2$  cathodes with a maximum specific capacity of  $\approx 16 \text{ mAh g}^{-1}$  and voltages of  $\approx 1 \text{ V}$ . These batteries can well be considered as respectable ones.

**Protonic and Electronic Conductance in Melanin:** The debate as to whether melanins were natural semiconductors was resolved in a series of papers by Mostert et al.<sup>[25,27,215]</sup> between 2009 and 2012, in which the authors showed the predominant charge carrier to be the proton. **Figure 19** is considered the definitive

evidence in this regard, whereby the hydration-dependent conductance (measured over millimeters) was closely correlated with proton transport signatures from the analogous muon spin relaxation spectroscopy analysis. The authors were also able to extract a muon hopping rate of  $\approx 0.3 \mu\text{s}^{-1}$  (a proxy for the proton hopping rate) which was consistent with proton transport mediated by the Grotthuss mechanism and proton diffusion mobilities consistent this mechanism as described in Section 2. It was proposed that a local equilibrium reaction (**Figure 20**—the comproportionation equilibrium) was responsible for driving the production of protons and the conversion between various quinone and hydroxyl quinone redox states. The macroscopic result of the comproportionation equilibrium are hydration-dependent proton and semiquinone spin populations which could in principle give rise to a mixed conduction.

This concept of melanins being mixed electronic–protonic conductors became the prevailing hypothesis with some notable contributions by Santato and co-workers<sup>[39,211]</sup> using electrochemical impedance spectroscopy (EIS) and current–voltage analysis on thin films of melanins produced under a variety of processing conditions. In particular, they found conductances of order  $10^{-3}$  to  $10^{-4} \text{ S cm}^{-1}$  in thin films, but did conclude this to be dominated by ionic effects at high hydration.<sup>[211]</sup> The same group also reported subtle electrochemical effects at melanin–electrode interfaces such as the formation of dendritic conducting tracks with gold electrodes.<sup>[38]</sup> This really emphasizes the fact that solid-state electrical measurements on materials that conduct ions and that are electrochemically active are fraught with complications. Most recently, Mostert et al.<sup>[216]</sup> have provided strong evidence using hydration-dependent photo-EPR (electron paramagnetic resonance) that the melanin system is essentially a protonic conducting matrix with no observable electronic component. This hypothesis was exemplified by Sheliakina et al.<sup>[40]</sup> who demonstrated the first all solid-state melanin-based organic electrochemical transistor (OECT). In this prototype bioelectronic interface (**Figure 21**), a proton conducting melanin gate was used to dedope a p-type organic semiconducting channel. The mechanism was proven to be volumetric, i.e., the device gated by the direct injection of protons into the semiconducting channel. As such, this OECT directly transduces electronic-to-protonic currents.

**Melanin Composites and Doping:** It has been known for several decades that melanins bind metal ions very strongly—particularly transition metals such as copper, iron and europium.<sup>[217–219]</sup> There is some evidence that this metal binding could perturb the macroscopic electrical conductance, but this is by no means definitive. The heterogeneity of melanins and the fact that they are proton transport systems, would tend to suggest that conventional doping precepts should be redundant. However, as the heme-doped BSA example (vide supra) demonstrates—solid-state doping in macromolecular systems is an emerging concept more akin to developments in molecular doping of organic semiconductors. Returning to the themes of this section in terms of material modification, there have been numerous attempts to incorporate or mix melanins into conducting matrices to create new functional systems. These include layer-by-layer assembled melanin–polyaniline biocompatible electrodes with conductivities of  $\approx 1 \text{ S cm}^{-1}$  at 24% by weight loading biopolymer,<sup>[220]</sup> poly(vinyl alcohol)–sepia melanin

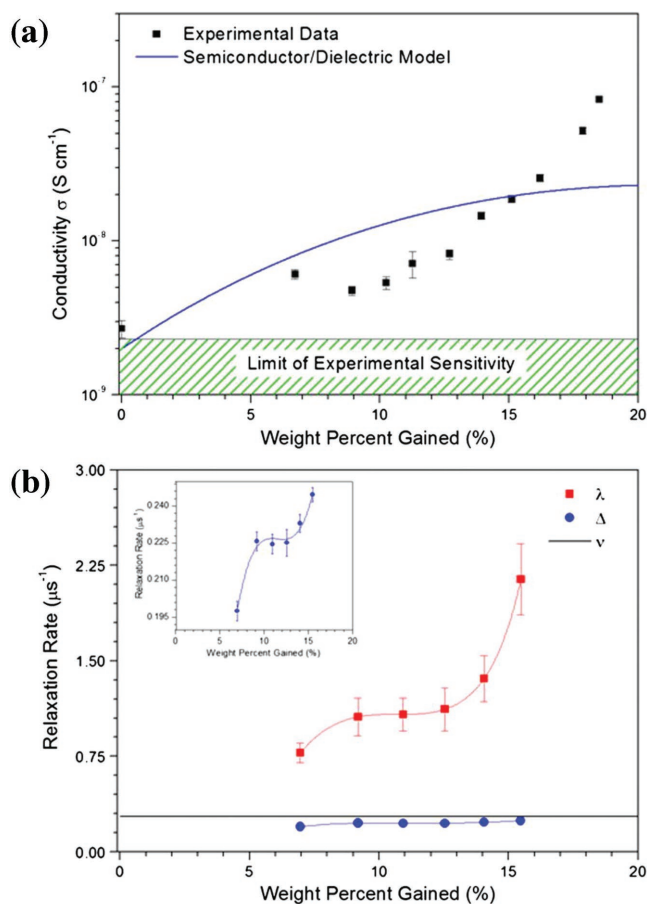


**Figure 19.** a) The conductance of a solid-state pellet of synthetic melanin as a function of water content. The line shows the best fit to a modified dielectric model assuming the system to be a semiconductor. b) Muon spin relaxation spectroscopy ( $\mu\text{SR}$ ): the paramagnetic and diamagnetic relaxation rates for melanin pellets as a function of water content. The muon hopping rate,  $\nu$ , was found to be constant at  $0.28 \pm 0.03 \mu\text{s}^{-1}$  (SE). The data confirms that carriers are generated with increased hydration as reflected for protons and electrons by  $\Delta$  and  $\lambda$ , respectively. Reproduced with permission.<sup>[27]</sup> Copyright 2012, National Academy of Sciences.

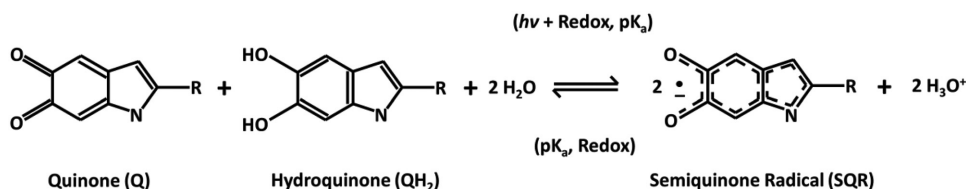


**Figure 20.** The redox equilibrium that produces charge carriers in melanin: the comproportionation equilibrium. Indolequinone moieties of varying oxidation states react with water to form hydronium and an intermediate state, the semiquinone radical. The light activated and dark activated mechanisms are summarized in the brackets. Reproduced with permission.<sup>[216]</sup> Copyright 2018, The Authors, published by Royal Society of Chemistry.

layer-by-layer nanocomposites for conductive anti-inflammatory coatings,<sup>[221]</sup> and melanin-PEDOT:PSS transparent conducting electrodes for organic light-emitting diodes.<sup>[222]</sup> To lesser or greater extents, these examples exemplify the motivation behind using melanins (and indeed other conducting

biocompatible materials)—the need to create electrically active interfaces to host and interact with living biological systems.

#### 4. Perspective and Future Directions

In the final part of our review, we discuss what conductive macroscale biomolecular materials can be good for, while trying to distinguish between the different materials that we have detailed above. Overall, conductive macroscale biomolecular materials can be considered as a small niche field within the wide field of organic electronics. The term “organic electronics” commonly refers to as organic semiconductors or conductive polymers. Though all of these terms are used interchangeably, we can try to distinguish between them by the type of material and the type of conduction. Organic semiconductor is perhaps the most used term and it refers to both polymers as well as crystalline material formed by small molecules. Nonetheless, and as inferred from their names, organic semiconductors are being explored only for their electron conduction. Ionic conducting materials, on the other hand, are usually polymers, and as such are more commonly referred to as conductive polymers. In the current discussion, we avoid complex terminology, and we divide the materials according to the type of the charge carrier and to the crystalline or amorphous nature. In this section, we present our perspective on the possible applications of conductive biomolecular materials. Before highlighting those applications that are well suited to some of the advantageous features of biomolecular materials, we briefly discuss what are likely *not* to be the main applications but are currently the most common for conducting organic materials. Perhaps the most studied application in recent decades for organic materials is their use as the light harvesting elements in organic photovoltaics (OPV).<sup>[223–225]</sup> Interestingly, one of the first (if not the first) OPV device was prepared in 1975 using a biomolecule, chlorophyll-a, which resulted in a poor efficiency of 0.001% (further discussed in Section 3.1.3).<sup>[108]</sup> Since then, the efficiencies of organic solar cells have progressively increased, up to the current state of the art of 12%.<sup>[226,227]</sup> The main rational and driving force of this field was the creation of low-cost all-carbon-based materials for PV with superior manufacturing throughput and mechanical flexibility. The second main application for organic semiconductors is in the field of organic light-emitting diodes (OLEDs). In this case, the organic semiconductor converts electricity to light at very respectable quantum efficiencies.<sup>[228–230]</sup> OLEDs have enjoyed considerable momentum in recent years and they already reached the point of worldwide commercial

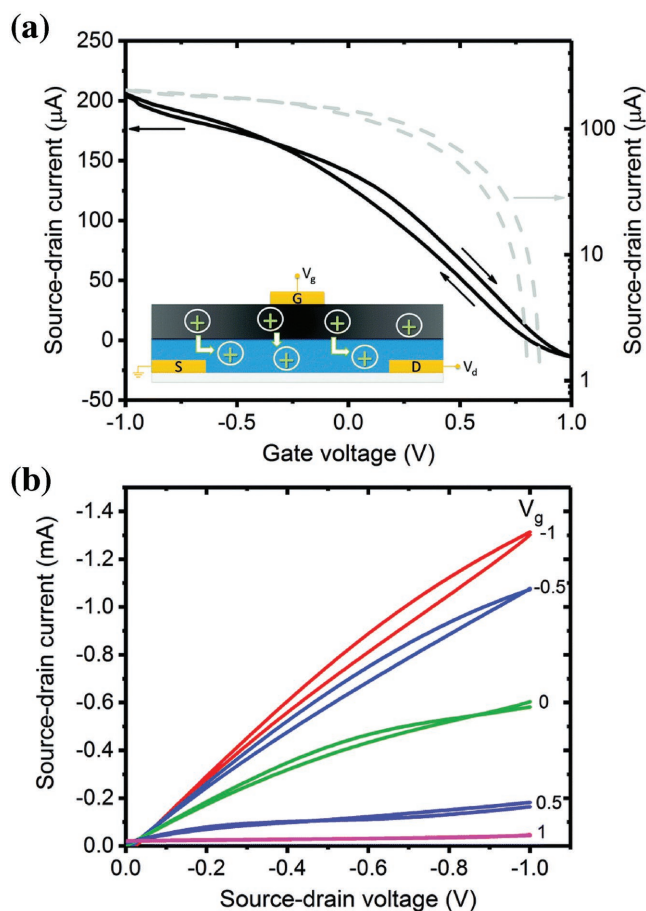


**Figure 21.** a) The transfer characteristics of a PEDOT:PSS transistor channel (with dimensions 100 nm thick, 100 μm channel length—inset shows the architecture with source (S), drain (D), and gate (G) electrodes) and a melanin top gate (gold gate electrode) in a solid-state organic electrochemical transistor configuration. Proton injection from the hydrated melanin top gate dedopes the PEDOT:PSS channel reducing the source–drain current and turning the transistor “off.” b) Transistor output characteristics confirming the operation shown in (a). Reproduced under the terms of the CC-BY License.<sup>[40]</sup> Copyright 2018, Royal Society of Chemistry.

implementation mainly in screens of smartphones and televisions. In both OPV and OLED applications, the charge transport pathways are not macroscopic being of order 100–1000 nm (i.e., the distance between electrodes in a thin film diode architecture). Due to the inferior electronic conductivity of biomolecular materials compared to organic semiconductors, their relatively poor processability and in some cases stability, we foresee little opportunity for biomolecular materials in these applications.

#### 4.1. Materials for Fuel Cells and Charge Storage

In this review, we have discussed both electron and ionic conduction. In addition to the latter common applications of organic electronics that exploited their electron conductivity, there is also substantial work directed to the utilization of organic ionomers. The most studied application in the field is the use of organic materials for the formation of proton-exchange membranes or polymer electrolyte membranes (both abbreviated as PEM) for the use in fuel cells.<sup>[231–233]</sup> Perhaps the most used organic ionomer for this application is Nafion (of DuPont), but many other sulfonated, fluorinated, carboxylated, or imide-based polymers have been used to this end.<sup>[231–233]</sup> The membrane has a crucial role in the fuel cell, which is to selectively transfer protons from the cell's anode to cathode. The conduction pathway in this application is on the micrometer length scale. Biomolecular ionomers have, in general, lower proton conductivity compared to other organic ionomers. Taken together with the necessity of some fuel cell application to operate at high temperature, biomolecular materials are not the most attractive option for this type of application.

An additional application for ionic conducting organic materials is charge storage applications and mainly for their integration in supercapacitors, which are high-capacity capacitors with specific energy of  $>1 \text{ Wh kg}^{-1}$ . There are two main categories of supercapacitors. The first is an electrostatic double layer capacitor, where carbon electrodes are used to store charges in the double layer interface between solution and electrode, which is on the nanometer scale. The second category of supercapacitor is an electrochemical pseudocapacitor, which stores charges within the bulk of a material as a result of electrochemical redox reactions. In the last 20 years, there has been considerable progress in using conductive organic materials for electrochemical pseudocapacitors due to their ability to be reduced and oxidized by an anion or a cation.<sup>[234]</sup> The redox of conductive organic materials is the same process for doping them, where anions are used for p-doping and cations for n-doping. As for today, the most used materials for this type of supercapacitors are all conducting polymers of either polypyrroles, polyaniline, or PEDOT (or other thiophene-based polymers). Similar to the latter, common conducting organic polymers have the potential to be electrochemically doped (p or n) with small ions.<sup>[235]</sup> Only in the last 4–5 years real progress has been made in trying to incorporate biomolecular conducting polymers into capacitance devices, whereas the main focus, though not exclusively, was on using melanins.<sup>[214,236–239]</sup>

While discussing charge storage applications, we should also briefly mention charge storage in memories, and especially

nonvolatile type of memories, where there were some attempts for the use of biomolecules as the charge storage media in memories.<sup>[212,240–242]</sup>

#### 4.2. Bioelectronics—Transduction and Logic

As discussed earlier in the review, the field of bioelectronics is presenting new opportunities and challenges for electronic materials, and particularly materials and device architectures that can sustain ionic/protonic currents, and that have intrinsic biocompatibility. Biological systems rely on ionic and molecular signaling pathways as opposed to processes relying on electronic transport. Thus, idealized bioelectronic interfaces must rely on ionic-to-electronic transduction. Traditional conducting polymers, such as PEDOT, have enabled unique ion pump technologies, allowing direct conversion of electronic to ionic signals.<sup>[243,244]</sup> Conducting polymers have already advanced to clinical applications for neural recording, giving the combined advantages of lower impedance and biocompatibility and conformability.<sup>[245,246]</sup> Biomaterials are uniquely poised to be the ideal candidates for bioelectronic interfaces, provided they satisfy the necessary demands for conductivity. Melanin is a candidate for a biomaterial replacement for synthetic conducting polymers currently used in devices. Melanin interfaces can promote neural cell growth and can be suitable for nerve tissue engineering and to improve recording electrode performance.<sup>[247]</sup> Processing of melanins with conductivity in the range of  $1\text{--}10 \text{ S cm}^{-1}$  could allow it to be a suitable modification layer for higher-performance neural recording and stimulation electrodes. The same applies for indigo-based materials, which have high mobility but low conductivity since they are not doped. Developing an effective doping strategy for indigos could make them effective for bioelectronics interfaces since recent work has shown that structured indigoid nanocrystals form intimate interfaces with cultured cells.<sup>[248]</sup> The concept of bioelectronic logic is beginning to emerge—stated simply, the ability to perform fundamental computational or processing tasks at the bioelectronic interface rather than remotely will reduce external connection complexities and dramatically expand functionality. The first prototype “bioelectronic logic” circuit elements based upon ion bipolar junction transistors and organic electrochemical transistors have been reported in the past decade,<sup>[249,250]</sup> but much more recently all-solid-state transistors that have the potential for large-scale integration have begun to emerge.<sup>[40,251]</sup> Processing frequency bandwidths of hundreds of kHz would be perfectly acceptable to drive and respond to nerve signaling and trans-membrane events, and this must be a primary target for bioelectronic logic element performance.

The role of long-range electronic and ionic transport—and indeed the efficient transduction between signals carried by electrons and ions—are important prerequisites of creating integrated bioelectronic logic. For example, one could imagine centimeter arrays of transducing and processing transistors targeting small clusters of neurons, reading synaptic signals, and applying complementary triggering to deliver corrective functionality. In this case, “ionic” wires capable of transporting carriers over macroscale dimensions at respectable mobilities would be needed to facilitate distributed processing. Likewise,

“light-based” signal delivery and transduction as envisaged in optogenetic schemes for neurostimulation or artificial vision would potentially need millimeter-scale proton-wire meshes and rapid electron transfer to stimulate the visual cortex through addressable light-emitting diode microarrays.<sup>[252]</sup> On the single-cell level, nanoparticles of melanins or indigoids can be used for transducing light into localized photothermal or photocapacitive events.<sup>[248,253]</sup> The biocompatibility of these materials strongly suggests further exploration of this topic.

At a more basic level, transduction between ionic and electronic currents at high fidelity with acceptable speed and signal-to-noise ratio is still an ongoing challenge. The requirement to perform these tasks in an all-solid-state and biocompatible system is a further layer of complexity. Understanding how to control and engineer ion transport through suitable media is central to this endeavor, and with only a few exceptions, electronic materials that can also sustain ionic currents remain elusive. In particular, n-type and p-type organic semiconductors whose conductance can be modulated by proton/ion doping and dedoping look like new avenues of opportunity for the creation of complementary transistor circuits.<sup>[254]</sup> It is probably the case though, given the intrinsic differences between the physics of ionic and electronic charge carriers (see also Table 1), that bioelectronic transducing interfaces will have separate conducting channels for electrons and ions, connected via a tailored hybrid medium. This seems to be the current thrust of the field as we search for new ways to mediate between the two disparate worlds of classical and quantum mechanical transport.

### 4.3. Cell Scaffolding Materials

While in previous sections we discussed common applications for an electron or ionic organic conductor, from this point we will start our discussion on relative niche fields, where we think a biomolecular conductive polymer can be considered as superior to other organic conductors, and we will start with biomedical applications. Tissue engineering is considered the future of regenerative medicine, which involves the formation of a tissue *in vitro*, and its implantation *in vivo* for the repair of an injured site, such as cartilage, heart (myocardial infarction), brain, and more. The formation of the tissue takes place on a certain scaffold, and accordingly, the field of biomaterials for cell scaffolding is highly active, where the most used types of materials for tissue engineering are hydrogels and electrospun mats. In recent years, several studies showed that the use of conductive scaffold might result in superior tissues, and especially for cardiac and neuronal tissue engineering.<sup>[255]</sup> In these studies, mainly conductive organic polymers, such as polyaniline or PEDOT,<sup>[256,257]</sup> have been used as the conductive part of the scaffold that was used for tissue engineering. However, since scaffolds for tissue engineering, and especially for cardiac and neurons, require an elastic deformable freestanding material, the use of the organic polymer was restricted for the coating or blending with another type of polymer, usually an elastomer, which is responsible for the mechanical properties of the final material. The latter type of material can be either an organic polymer, such as polyethylene-glycol, but it can also be a biomolecular polymer. The formation of conductive blended

polymers composed of a biomolecular polymer together with an organic conductor one is discussed in detail above (Section 3.2). Several works used conductive biomolecular polymers, and mainly collagen-, gelatin-, or chitosan-based ones, for cardiac and neuronal tissue engineering applications.<sup>[258–268]</sup> Indeed, in most of these studies, the biomolecular polymer was mixed or coated with a traditional organic conductive polymer, and in a few studies, carbon nanotubes were blended into the biomolecular polymer for enabling the electrical conductivity. Among the various example, one stands out as being purely biomolecular, where porphyrins were incorporated into a protein-based material for neuronal tissue engineering.<sup>[268]</sup> The latter study also shows that the scaffold can be formed from a most abundant blood serum protein, which means that the scaffold can be prepared from the proteins of a specific patient (*i.e.*, autologous source), which paves the way for personalized tissue engineering. It is not clear yet what is the exact mechanism in which a conductive substrate affects the growth of the tissue, and trying to explain it is not in the scope here, but it is clear that for *in vivo* applications, an all biomolecular-based polymer has a big advantage due to the outcome of its biodegradation. Hence, we foresee that for this type of application, the use of biomolecular conductive polymers might prove itself very useful. Since for tissue engineering applications there is a need for a freestanding, flexible, and most often viscoelastic type of material, the protein-based or polysaccharide-based types of biomolecular polymers are the most suitable candidates.

### 4.4. Artificial Photosynthetic Platforms and Model Studies on Ionic Conduction

In this last section, we are returning to the beginning of the Introduction, and to our main rationale in choosing biological materials as charge conductors. As stated earlier, electrons in biology are being mediated by cofactors, such as porphyrins, which are located within proteins. Ions are transferred usually across specific transmembrane protein channels. In photosynthesis, there is an additional process of energy transfer, also between cofactors within proteins, for mediating the excited-state electron to the start of the electron transport chain reaction. The high efficiency of the photosynthetic system in mediating charges has resulted in a substantial effort in using the principles in photo-electrochemical cells.<sup>[269,270]</sup> In these latter works, the authors utilized the electron charge separation of the photosynthetic process for the generation of electrical current or for water splitting and hydrogen evolution. Biomolecular materials can also be used for the formation of completely new artificial photosynthetic-like system in order to explore the factors associated with long-range energy or electron transfer across cofactors. For instance, DNA was used as a scaffold for binding molecular cofactors for the formation of artificial energy transfer relay, which allowed exploration of the role of spatial organization and packing density of the cofactors in mediating the energy.<sup>[271]</sup> Nonetheless, the latter study used DNA as the scaffold, which is not the natural material for mediating charges, as well as the dimensions of the systems were limited. Using protein-based materials for this type of artificial system has two main advantages, first, it will imitate natural

energy/electron transfer, and second, it will allow analysis of the energy/electron transfer over longer distances. As already mentioned, proteins doped with natural cofactors already show very long-range electron transfer,<sup>[207]</sup> but further scientific effort is needed now to better control the density and location of the cofactors within the protein-based material. Hence, we believe that protein-based macroscopic structures can be used as an ideal type of material to explore the factors associated with biological electron/energy transfer.

The use of conductive biomolecular materials can also contribute to our better understanding of how ions flow across biological interfaces and junctions. As stated, ionic conduction is fundamental in many biological processes. However, deciphering the factors associated with the ionic conduction and the mechanism of proton transfer is a complicated endeavor. In this review, we mainly focused on protonic conductivity, and we believe that macroscopic protein- or peptide-based structures can vastly contribute to our understanding of natural proton conduction. For instance, and as discussed above, films of the reflectin protein as well as self-assembled structure of amyloid-like peptides were used to decipher the role of a certain amino acid in the proton conduction mechanism.<sup>[190,202,272]</sup>

## 5. Future Directions and Final Comments

Here, we have “bridged” the worlds of charge conduction in biology and our recent technological achievements in creating modern electronics. The physics of the signal-carrying entities in these two arenas are radically different and connect through small and large molecule organic conductors and semiconductors. As always, our attempts to create technology and understand underlying principles are often guided by models in the natural world. Likewise, as we seek to gain new insight into natural processes, we can utilize artificial models—and that is precisely how the field of macroscale electrical transport in biomolecules has evolved: proteins, synthetic polymers, DNA, melanins, porphyrins, etc., are mixed and merged to create new understanding and technological opportunities. Bioinspired functional electrical materials are a direct example of where technology can learn from the natural world. We have also highlighted a number of perspective applications where biomolecular ionics and electronics may make a significant impact—in particular information and energy storage, and the biotic/abiotic interface as we seek to communicate, engineer, and control biological processes. Bioelectronics and in situ biosensing are “new horizons” linked to the exciting concept of individually tailored nanomedicines and the next wave of health therapies. Finally, as traditional discipline silos crumble, the field of biomolecular ionics and electronics is a clear example of multidisciplinary frontier science mixing materials, electrical engineering, physics, chemistry, and biology.

## Acknowledgements

N.A. thanks the Chaya Career Advancement Chair, the Russel Berrie Nanotechnology Institute, and the Grand Technion Energy Program for financial support. P.M. is a Sêr Cymru Research Chair funded through

the Sêr Cymru II Program (European Regional Development Fund and Welsh European Funding Office) and Swansea University via the Sustainable Advanced Materials Program.

## Conflict of Interest

The authors declare no conflict of interest.

## Keywords

bioelectronics, biomaterials, conductive polymers, electron conduction, proton conduction

Received: April 8, 2018

Revised: June 25, 2018

Published online: October 17, 2018

- [1] J. N. Onuchic, D. N. Beratan, J. R. Winkler, H. B. Gray, *Annu. Rev. Biophys. Biomol. Struct.* **1992**, *21*, 349.
- [2] G. B. Khomutov, L. V. Belovolova, S. P. Gubin, V. V. Khanin, A. Y. Obydenov, A. N. Sergeev-Cherenkov, E. S. Soldatov, A. S. Trifonov, *Bioelectrochemistry* **2002**, *55*, 177.
- [3] J. W. Zhao, J. J. Davis, *Nanotechnology* **2003**, *14*, 1023.
- [4] X. Y. Xiao, B. Q. Xu, N. J. Tao, *J. Am. Chem. Soc.* **2004**, *126*, 5370.
- [5] N. Amdursky, *ChemPlusChem* **2015**, *80*, 1075.
- [6] N. Amdursky, D. Marchak, L. Sepunaru, I. Pecht, M. Sheves, D. Cahen, *Adv. Mater.* **2014**, *26*, 7142.
- [7] M. Taniguchi, T. Kawai, *Physica E* **2006**, *33*, 1.
- [8] E. Braun, Y. Eichen, U. Sivan, G. Ben-Yoseph, *Nature* **1998**, *391*, 775.
- [9] A. J. Storm, J. v. Noort, S. d. Vries, C. Dekker, *Appl. Phys. Lett.* **2001**, *79*, 3881.
- [10] A. Y. Kasumov, M. Kociak, S. Gueron, B. Reulet, V. T. Volkov, D. V. Klinov, H. Bouchiat, *Science* **2001**, *291*, 280.
- [11] G. H. Moe-Behrens, *Comput. Struct. Biotechnol. J.* **2013**, *7*, 1.
- [12] G. Kemeny, B. Rosenberg, *J. Chem. Phys.* **1970**, *53*, 3549.
- [13] M. R. Powell, B. Rosenberg, *Biopolymers* **1970**, *9*, 1403.
- [14] B. Rosenberg, *J. Chem. Phys.* **1962**, *36*, 816.
- [15] J. E. McGinness, *Science* **1972**, *177*, 896.
- [16] J. McGinness, P. Corry, P. Proctor, *Science* **1974**, *183*, 853.
- [17] N. S. Malvankar, G. M. King, D. R. Lovley, *ISME J.* **2015**, *9*, 527.
- [18] N. S. Malvankar, D. R. Lovley, *ChemSusChem* **2012**, *5*, 1039.
- [19] N. S. Malvankar, M. Vargas, K. P. Nevin, A. E. Franks, C. Leang, B.-C. Kim, K. Inoue, T. Mester, S. F. Covalla, J. P. Johnson, V. M. Rotello, M. T. Tuominen, D. R. Lovley, *Nat. Nanotechnol.* **2011**, *6*, 573.
- [20] G. Reguera, K. D. McCarthy, T. Mehta, J. S. Nicoll, M. T. Tuominen, D. R. Lovley, *Nature* **2005**, *435*, 1098.
- [21] M. Y. El-Naggar, G. Wanger, K. M. Leung, T. D. Yuzvinsky, G. Southam, J. Yang, W. M. Lau, K. H. Nealson, Y. A. Gorby, *Proc. Natl. Acad. Sci. USA* **2010**, *107*, 18127.
- [22] K. M. Leung, G. Wanger, M. Y. El-Naggar, Y. Gorby, G. Southam, W. M. Lau, J. Yang, *Nano Lett.* **2013**, *13*, 2407.
- [23] C. Pfeffer, S. Larsen, J. Song, M. Dong, F. Besenbacher, R. L. Meyer, K. U. Kjeldsen, L. Schreiber, Y. A. Gorby, M. Y. El-Naggar, K. M. Leung, A. Schramm, N. Risgaard-Petersen, L. P. Nielsen, *Nature* **2012**, *491*, 218.
- [24] R. Y. Adhikari, N. S. Malvankar, M. T. Tuominen, D. R. Lovley, *RSC Adv.* **2016**, *6*, 8354.
- [25] A. Bernardus Mostert, B. J. Powell, I. R. Gentle, P. Meredith, *Appl. Phys. Lett.* **2012**, *100*, 093701.



- [26] P. Meredith, T. Sarna, *Pig. Cell Melanoma Res.* **2006**, *19*, 572.
- [27] A. B. Mostert, B. J. Powell, F. L. Pratt, G. R. Hanson, T. Sarna, I. R. Gentle, P. Meredith, *Proc. Natl. Acad. Sci. USA* **2012**, *109*, 8943.
- [28] A. Pullman, B. Pullman, *Biochim. Biophys. Acta* **1961**, *54*, 384.
- [29] A. M. Potts, P. C. Au, *Exp. Eye Res.* **1976**, *22*, 487.
- [30] E. Trukhan, N. Perevozchikov, M. Ostrovskii, *Biofizika* **1970**, *15*, 1052.
- [31] B. Rosenberg, E. Postow, *Ann. N. Y. Acad. Sci.* **1969**, *158*, 161.
- [32] M. R. Powell, B. Rosenberg, *J. Bioenerg.* **1970**, *1*, 493.
- [33] P. Crippa, V. t. Cristofaletti, N. Romeo, *Biochim. Biophys. Acta, Gen. Subj.* **1978**, *538*, 164.
- [34] T. Strzelecka, *Physiol. Chem. Phys.* **1982**, *14*, 219.
- [35] T. Strzelecka, *Physiol. Chem. Phys.* **1982**, *14*, 223.
- [36] M. Da Silva, S. Deziderio, J. Gonzalez, C. Graeff, M. Cotta, *J. Appl. Phys.* **2004**, *96*, 5803.
- [37] M. M. Jastrzebska, H. Isotalo, J. Paloheimo, H. Stubb, *J. Biomater. Sci., Polym. Ed.* **1996**, *7*, 577.
- [38] J. Wünsche, L. Cardenas, F. Rosei, F. Ciccoira, R. Gauvin, C. F. Graeff, S. Poulin, A. Pezzella, C. Santato, *Adv. Funct. Mater.* **2013**, *23*, 5591.
- [39] J. Wünsche, Y. Deng, P. Kumar, E. Di Mauro, E. Josberger, J. Sayago, A. Pezzella, F. Soavi, F. Ciccoira, M. Rolandi, C. Santato, *Chem. Mater.* **2015**, *27*, 436.
- [40] M. Sheliakina, A. Mostert, P. Meredith, *Mater. Horiz.* **2018**, *5*, 256.
- [41] P. Meredith, C. Bettinger, M. Irimia-Vladu, A. Mostert, P. Schwenn, *Rep. Prog. Phys.* **2013**, *76*, 034501.
- [42] R. C. Agrawal, R. K. Gupta, *J. Mater. Sci.* **1999**, *34*, 1131.
- [43] Y. Yung-Fang Yu, J. T. Kummer, *J. Inorg. Nucl. Chem.* **1967**, *29*, 2453.
- [44] B. B. Owens, G. R. Argue, *Science* **1967**, *157*, 308.
- [45] P. V. Wright, *Br. Poly. J.* **1975**, *7*, 319.
- [46] B. B. Owens, *J. Power Sources* **2000**, *90*, 2.
- [47] M. S. Whittingham, *Science* **1976**, *192*, 1126.
- [48] K. T. Adjemian, S. J. Lee, S. Srinivasan, J. Benziger, A. B. Bocarsly, *J. Electrochem. Soc.* **2002**, *149*, A256.
- [49] F. Damay, L. C. Klein, *Solid State Ionics* **2003**, *162*, 261.
- [50] N. Y. Jia, M. C. Lefebvre, J. Halfyard, Z. G. Qi, P. G. Pickup, *Electrochem. Solid-State Lett.* **2000**, *3*, 529.
- [51] Z. G. Shao, P. Joghee, I. M. Hsing, *J. Membr. Sci.* **2004**, *229*, 43.
- [52] D. D. Eley, R. B. Leslie, in *Advances in Chemical Physics*, Vol. VII (Ed: J. Duchesne), John Wiley & Sons, Inc., New York **1964**, pp. 238–258.
- [53] D. Eley, D. Spivey, *Trans. Faraday Soc.* **1962**, *58*, 411.
- [54] D. Eley, D. Spivey, *Trans. Faraday Soc.* **1960**, *56*, 1432.
- [55] E. Murphy, *J. Phys. Chem. Solids* **1960**, *16*, 115.
- [56] E. Murphy, *J. Phys. Chem. Solids* **1960**, *15*, 66.
- [57] D. Porath, A. Bezryadin, S. de Vries, C. Dekker, *Nature* **2000**, *403*, 635.
- [58] P. Fulde, *Electron Correlations in Molecules and Solids*, Springer, Heidelberg, Germany **1995**.
- [59] R. G. Endres, D. L. Cox, R. R. Singh, *Rev. Mod. Phys.* **2004**, *76*, 195.
- [60] P. P. Kumar, S. Yashonath, *J. Chem. Sci.* **2006**, *118*, 135.
- [61] L. Glasser, *Chem. Rev.* **1975**, *75*, 21.
- [62] S. Walbran, A. Kornyshev, *J. Chem. Phys.* **2001**, *114*, 10039.
- [63] N. Agmon, *Chem. Phys. Lett.* **1995**, *244*, 456.
- [64] G. Careri, A. Giansanti, J. A. Rupley, *Proc. Natl. Acad. Sci. USA* **1986**, *83*, 6810.
- [65] I. Riess, *Solid State Ionics* **2000**, *136*, 1119.
- [66] C. Zhong, Y. Deng, A. F. Roudsari, A. Kapetanovic, M. P. Anantram, M. Rolandi, *Nat. Commun.* **2011**, *2*, 476.
- [67] N. F. Mott, E. A. Davis, *Electronic Processes in Non-Crystalline Materials*, Oxford University Press, Oxford **1979**.
- [68] E. S. Ferreira, A. N. Hulme, H. McNab, A. Quye, *Chem. Soc. Rev.* **2004**, *33*, 329.
- [69] M. Seefelder, *Indigo in Culture, Science, and Technology*, Ecomed, Landsberg, Germany **1994**.
- [70] E. D. Głowacki, G. Voss, N. S. Sariciftci, *Adv. Mater.* **2013**, *25*, 6783.
- [71] T. Bechtold, R. Mussak, *Handbook of Natural Colorants*, John Wiley & Sons, Chichester, UK **2009**.
- [72] E. Steingruber, *Indigo Colorants, Ullmann's Encyclopedia of Industrial Chemistry*, Wiley-VCH, Weinheim, Germany **2007**.
- [73] A. M. Bond, F. Marken, E. Hill, R. G. Compton, H. Hügel, *J. Chem. Soc., Perkin Trans. 2* **1997**, 1735.
- [74] A. Roessler, O. Dossenbach, P. Rys, W. Marte, *J. Appl. Electrochem.* **2002**, *32*, 647.
- [75] A. Vuorema, P. John, M. Keskitalo, M. A. Kulandainathan, F. Marken, *Dyes Pigment.* **2008**, *76*, 542.
- [76] R. Rondao, J. S. Seixas de Melo, V. D. B. Bonifácio, M. J. Melo, *J. Phys. Chem. A* **2010**, *114*, 1699.
- [77] M. M. Lezhnina, T. Grewe, H. Stoehr, U. Kynast, *Angew. Chem., Int. Ed.* **2012**, *51*, 10652.
- [78] J. Seixas de Melo, R. Rondão, H. Burrows, M. Melo, S. Navaratnam, R. Edge, G. Voss, *J. Phys. Chem. A* **2006**, *110*, 13653.
- [79] M. Dittmann, F. F. Graupner, B. Maerz, S. Oesterling, R. de Vivie-Riedle, W. Zinth, M. Engelhard, W. Lüttke, *Angew. Chem., Int. Ed.* **2014**, *53*, 591.
- [80] J. Pina, M. Alnady, A. Eckert, U. Scherf, J. S. S. de Melo, *Mater. Chem. Front.* **2018**, *2*, 281.
- [81] J. Pina, D. Sarmento, M. Accoto, P. L. Gentili, L. Vaccaro, A. Galvão, J. S. Seixas de Melo, *J. Phys. Chem. B* **2017**, *121*, 2308.
- [82] E. D. Głowacki, G. Voss, K. Demirak, M. Havlicek, N. Sünger, A. C. Okur, U. Monkowius, J. Gąsiorowski, L. Leonat, N. S. Sariciftci, *Chem. Commun.* **2013**, *49*, 6063.
- [83] E. Głowacki, D. Apaydin, Z. Bozkurt, U. Monkowius, K. Demirak, E. Tordin, M. Himmelsbach, C. Schwarzinger, M. Burian, R. Lechner, *J. Mater. Chem. C* **2014**, *2*, 8089.
- [84] M. Sytnyk, E. D. Głowacki, S. Yakunin, G. Voss, W. Schöfberger, D. Kriegner, J. Stangl, R. Trotta, C. Gollner, S. Tollabimazraehno, *J. Am. Chem. Soc.* **2014**, *136*, 16522.
- [85] I. Sultana, M. Rahman, J. Wang, C. Wang, G. G. Wallace, H.-K. Liu, *Solid State Ionics* **2012**, *215*, 29.
- [86] M. Yao, K. Kuratani, T. Kojima, N. Takeichi, H. Senoh, T. Kiyobayashi, *Sci. Rep.* **2014**, *4*, 3650.
- [87] K. Uehara, K. Takagishi, M. Tanaka, *Solar Cells* **1987**, *22*, 295.
- [88] M. Irimia-Vladu, E. D. Głowacki, P. A. Troshin, G. Schwabegger, L. Leonat, D. K. Susarova, O. Krystal, M. Ullah, Y. Kanbur, M. A. Bodea, *Adv. Mater.* **2012**, *24*, 375.
- [89] O. Pitayatanakul, T. Higashino, T. Kadoya, M. Tanaka, H. Kojima, M. Ashizawa, T. Kawamoto, H. Matsumoto, K. Ishikawa, T. Mori, *J. Mater. Chem. C* **2014**, *2*, 9311.
- [90] E. D. Głowacki, L. Leonat, G. Voss, M.-A. Bodea, Z. Bozkurt, A. M. Ramil, M. Irimia-Vladu, S. Bauer, N. S. Sariciftci, *AIP Adv.* **2011**, *1*, 042132.
- [91] Y. Kanbur, M. Irimia-Vladu, E. D. Głowacki, G. Voss, M. Baumgartner, G. Schwabegger, L. Leonat, M. Ullah, H. Sarica, S. Erten-Ela, *Org. Electron.* **2012**, *13*, 919.
- [92] I. V. Klimovich, L. Leshanskaya, S. Troyanov, D. Anokhin, D. Novikov, A. Piryazev, D. Ivanov, N. Dremova, P. Troshin, *J. Mater. Chem. C* **2014**, *2*, 7621.
- [93] D. V. Anokhin, L. I. Leshanskaya, A. A. Piryazev, D. K. Susarova, N. N. Dremova, E. V. Shcheglov, D. A. Ivanov, V. F. Razumov, P. A. Troshin, *Chem. Commun.* **2014**, *50*, 7639.
- [94] B. Scherwitzl, R. Resel, A. Winkler, *J. Chem. Phys.* **2014**, *140*, 184705.
- [95] M. Truger, O. M. Roscioni, C. Röthel, D. Kriegner, C. Simbrunner, R. Ahmed, E. D. Głowacki, J. Simbrunner, I. Salzmänn, A. M. Coclite, *Cryst. Growth Des.* **2016**, *16*, 3647.
- [96] L. I. Leshanskaya, I. V. Klimovich, D. D. Dashitsyrenova, L. A. Frolova, E. S. Ershova, V. A. Sergeeva, V. Y. Tabakov, S. V. Kostyuk, K. A. Lyssenko, P. A. Troshin, *Adv. Opt. Mater.* **2017**, *5*.

- [97] E. F. Paulus, F. J. Leusen, M. U. Schmidt, *CrystEngComm* **2007**, *9*, 131.
- [98] E. D. Głowacki, M. Irimia-Vladu, M. Kaltenbrunner, J. Gsiorowski, M. S. White, U. Monkowius, G. Romanazzi, G. P. Suranna, P. Mastrotrilli, T. Sekitani, *Adv. Mater.* **2013**, *25*, 1563.
- [99] M. Jakešová, D. H. Apaydin, M. Sytnyk, K. Oppelt, W. Heiss, N. S. Sariciftci, E. D. Głowacki, *Adv. Funct. Mater.* **2016**, *26*, 5248.
- [100] E. Ehrenfreund, D. Moses, A. Heeger, J. Cornil, J. Bredas, *Chem. Phys. Lett.* **1992**, *196*, 84.
- [101] M. Irimia-Vladu, P. A. Troshin, M. Reisinger, G. Schwabegger, M. Ullah, R. Schwödiauer, A. Mumyatov, M. Bodea, J. W. Fergus, V. F. Razumov, *Org. Electron.* **2010**, *11*, 1974.
- [102] M. Irimia-Vladu, P. A. Troshin, M. Reisinger, L. Shmygleva, Y. Kanbur, G. Schwabegger, M. Bodea, R. Schwödiauer, A. Mumyatov, J. W. Fergus, *Adv. Funct. Mater.* **2010**, *20*, 4069.
- [103] E. D. Glowacki, L. Leonat, G. Voss, M. Bodea, Z. Bozkurt, M. Irimia-Vladu, S. Bauer, N. S. Sariciftci, in *Organic Semiconductors in Sensors and Bioelectronics IV*, Vol. 8118 (Eds: R. Shinar, I. Kymissis), International Society for Optics and Photonics, San Diego, CA, USA **2011**, p. 81180M.
- [104] F. Yakuphanoglu, M. Aydin, T. Kiliçoğlu, *J. Phys. Chem. B* **2006**, *110*, 9782.
- [105] X.-F. Wang, L. Wang, Z. Wang, Y. Wang, N. Tamai, Z. Hong, J. Kido, *J. Phys. Chem. C* **2013**, *117*, 804.
- [106] T. Zhuang, S.-i. Sasaki, T. Ikeuchi, J. Kido, X.-F. Wang, *RSC Adv.* **2015**, *5*, 45755.
- [107] A. Terenin, E. Putzeiko, I. Akimov, *Discuss. Faraday Soc.* **1959**, *27*, 83.
- [108] C. W. Tang, A. C. Albrecht, *J. Chem. Phys.* **1975**, *62*, 2139.
- [109] I. Lundström, G. A. Corker, M. Stenberg, *J. Appl. Phys.* **1978**, *49*, 701.
- [110] O. Inganäs, I. Lundström, *Thin Solid Films* **1981**, *85*, 129.
- [111] H. Kassi, S. Barazzouk, M. Brullemans, R. M. Leblanc, S. Hotchandani, *Thin Solid Films* **2010**, *518*, 5345.
- [112] S. Duan, G. Chen, M. Li, G. Chen, X.-F. Wang, H. Tamiaki, S.-i. Sasaki, *J. Photochem. Photobiol., A* **2017**, *347*, 49.
- [113] S.-W. Hwang, H. Tao, D.-H. Kim, H. Cheng, J.-K. Song, E. Rill, M. A. Brenckle, B. Panilaitis, S. M. Won, Y.-S. Kim, *Science* **2012**, *337*, 1640.
- [114] R. E. Barker, C. R. Thomas, *J. Appl. Phys.* **1964**, *35*, 87.
- [115] Y. Wan, K. A. M. Creber, B. Peppley, V. T. Bui, *Polymer* **2003**, *44*, 1057.
- [116] E. E. Josberger, P. Hassanzadeh, Y. Deng, J. Sohn, M. J. Rego, C. T. Amemiya, M. Rolandi, *Sci. Adv.* **2016**, *2*, e1600112.
- [117] J. Ma, Y. Sahai, *Carbohydr. Polym.* **2013**, *92*, 955.
- [118] K. Soontarapa, U. Intra, *Chem. Eng. Commun.* **2006**, *193*, 855.
- [119] P. Mukoma, B. R. Jooste, H. C. M. Vosloo, *J. Power Sources* **2004**, *136*, 16.
- [120] Y. Xiang, M. Yang, Z. Guo, Z. Cui, *J. Membr. Sci.* **2009**, *337*, 318.
- [121] B. Smitha, D. A. Devi, S. Sridhar, *Int. J. Hydrogen Energy* **2008**, *33*, 4138.
- [122] A. S. A. Khair, R. Puteh, A. K. Arof, *Physica B* **2006**, *373*, 23.
- [123] S. R. Majid, A. K. Arof, *Polym. Adv. Technol.* **2009**, *20*, 524.
- [124] V. V. Binsu, R. K. Nagarale, V. K. Shahi, P. K. Ghosh, *React. Funct. Polym.* **2006**, *66*, 1619.
- [125] Y. Wan, B. Peppley, K. A. M. Creber, V. T. Bui, E. Halliop, *J. Power Sources* **2008**, *185*, 183.
- [126] J. Wang, R. He, Q. Che, *J. Colloid Interface Sci.* **2011**, *361*, 219.
- [127] Y. Deng, B. A. Helms, M. Rolandi, *J. Polym. Sci., Part A: Polym. Chem.* **2015**, *53*, 211.
- [128] Y. Deng, E. Josberger, J. Jin, A. F. Roudsari, B. A. Helms, C. Zhong, M. P. Anantram, M. Rolandi, *Sci. Rep.* **2013**, *3*, 2481.
- [129] J. F. Du, Y. Bai, W. Y. Chu, L. J. Qiao, *J. Polym. Sci., Part B: Polym. Phys.* **2010**, *48*, 880.
- [130] E. L. Chávez, R. Oviedo-Roa, G. Contreras-Pérez, J. M. Martínez-Magadán, F. L. Castillo-Alvarado, *Int. J. Hydrogen Energy* **2010**, *35*, 12141.
- [131] M. H. Buraidah, A. K. Arof, *J. Non-Cryst. Solids* **2011**, *357*, 3261.
- [132] B. Smitha, S. Sridhar, A. A. Khan, *J. Appl. Polym. Sci.* **2005**, *95*, 1154.
- [133] S. Meenakshi, S. D. Bhat, A. K. Sahu, P. Sridhar, S. Pitchumani, A. K. Shukla, *J. Appl. Polym. Sci.* **2012**, *124*, E73.
- [134] B. Smitha, S. Sridhar, A. A. Khan, *Macromolecules* **2004**, *37*, 2233.
- [135] T. Gümüšoğlu, G. A. Arı, H. Deligöz, *J. Membr. Sci.* **2011**, *376*, 25.
- [136] M. M. Hasani-Sadrabadi, E. Dashtimoghadam, F. S. Majedi, K. Kabiri, M. Solati-Hashjin, H. Moaddel, *J. Membr. Sci.* **2010**, *365*, 286.
- [137] M. M. Hasani-Sadrabadi, E. Dashtimoghadam, F. S. Majedi, K. Kabiri, N. Mokarram, M. Solati-Hashjin, H. Moaddel, *Chem. Commun.* **2010**, *46*, 6500.
- [138] H. Lin, C. Zhao, W. Ma, H. Li, H. Na, *J. Membr. Sci.* **2009**, *345*, 242.
- [139] H. Zhang, H. Huang, P. K. Shen, *Int. J. Hydrogen Energy* **2012**, *37*, 6875.
- [140] S. Mohanapriya, A. K. Sahu, S. D. Bhat, S. Pitchumani, P. Sridhar, C. George, N. Chandrakumar, A. K. Shukla, *J. Electrochem. Soc.* **2011**, *158*, B1319.
- [141] B. P. Tripathi, V. K. Shahi, *Prog. Polym. Sci.* **2011**, *36*, 945.
- [142] B. Fugetsu, E. Sano, M. Sunada, Y. Sambongi, T. Shibuya, X. S. Wang, T. Hiraki, *Carbon* **2008**, *46*, 1256.
- [143] S. H. Yoon, H. J. Jin, M. C. Kook, Y. R. Pyun, *Biomacromolecules* **2006**, *7*, 1280.
- [144] Y. Y. Feng, X. Q. Zhang, Y. T. Shen, K. Yoshino, W. Feng, *Carbohydr. Polym.* **2012**, *87*, 644.
- [145] W. L. Hu, S. Y. Chen, Z. H. Yang, L. T. Liu, H. P. Wang, *J. Phys. Chem. B* **2011**, *115*, 8453.
- [146] J. A. Marins, B. G. Soares, K. Dahmouche, S. J. L. Ribeiro, H. Barud, D. Bonemer, *Cellulose* **2011**, *18*, 1285.
- [147] L. Dall'Acqua, C. Tonin, R. Peila, F. Ferrero, M. Catellani, *Synth. Met.* **2004**, *146*, 213.
- [148] H. H. Wang, L. Y. Bian, P. P. Zhou, J. Tang, W. H. Tang, *J. Mater. Chem. A* **2013**, *1*, 578.
- [149] J. H. Johnston, F. M. Kelly, J. Moraes, T. Borrmann, D. Flynn, *Curr. Appl. Phys.* **2006**, *6*, 587.
- [150] A. Tiwari, V. Singh, *eXPRESS Polym. Lett.* **2007**, *1*, 308.
- [151] A. Ramaprasad, V. Rao, *Sens. Actuators, B* **2010**, *148*, 117.
- [152] A. Ramaprasad, V. Rao, *Synth. Met.* **2008**, *158*, 1047.
- [153] N. Singh, K. K. Koziol, J. Chen, A. J. Patil, J. W. Gilman, P. C. Trulove, W. Kafienah, S. S. Rahatekar, *Green Chem.* **2013**, *15*, 1192.
- [154] X. Kang, J. Wang, H. Wu, I. A. Aksay, J. Liu, Y. Lin, *Biosens. Bioelectron.* **2009**, *25*, 901.
- [155] J. Jin, D. Lee, H.-G. Im, Y. C. Han, E. G. Jeong, M. Rolandi, K. C. Choi, B.-S. Bae, *Adv. Mater.* **2016**, *28*, 5169.
- [156] Z. Fang, H. Zhu, Y. Yuan, D. Ha, S. Zhu, C. Preston, Q. Chen, Y. Li, X. Han, S. Lee, G. Chen, T. Li, J. Munday, J. Huang, L. Hu, *Nano Lett.* **2014**, *14*, 765.
- [157] M. A. Daniele, A. J. Knight, S. A. Roberts, K. Radom, J. S. Erickson, *Adv. Mater.* **2015**, *27*, 1600.
- [158] Y. H. Jung, T.-H. Chang, H. Zhang, C. Yao, Q. Zheng, V. W. Yang, H. Mi, M. Kim, S. J. Cho, D.-W. Park, H. Jiang, J. Lee, Y. Qiu, W. Zhou, Z. Cai, S. Gong, Z. Ma, **2015**, *6*, 7170.
- [159] E. Murphy, *J. Colloid Interface Sci.* **1976**, *54*, 400.
- [160] G. H. Bardelmeyer, *Biopolymers* **1973**, *12*, 2289.
- [161] G. H. Bardelmeyer, *Biopolymers* **1973**, *12*, 2303.
- [162] T. E. DeCoursey, *Physiol. Rev.* **2003**, *83*, 475.
- [163] P. Leiderman, D. Huppert, N. Agmon, *Biophys. J.* **2006**, *90*, 1009.
- [164] L.-D. Koh, Y. Cheng, C.-P. Teng, Y.-W. Khin, X.-J. Loh, S.-Y. Tee, M. Low, E. Ye, H.-D. Yu, Y.-W. Zhang, M.-Y. Han, *Prog. Polym. Sci.* **2015**, *46*, 86.
- [165] S. Tsukada, H. Nakashima, K. Torimitsu, *PLoS One* **2012**, *7*, e33689.

- [166] Y. Xia, L. Yun, *Compos. Sci. Technol.* **2008**, *68*, 1471.
- [167] R. K. Pal, A. A. Farghaly, C. Wang, M. M. Collinson, S. C. Kundu, V. K. Yadavalli, *Biosens. Bioelectron.* **2016**, *81*, 294.
- [168] I. Cucchi, A. Boschi, C. Arosio, F. Bertini, G. Freddi, M. Catellani, *Synth. Met.* **2009**, *159*, 246.
- [169] I. S. Romero, N. P. Bradshaw, J. D. Larson, S. Y. Severt, S. J. Roberts, M. L. Schiller, J. M. Leger, A. R. Murphy, *Adv. Funct. Mater.* **2014**, *24*, 3866.
- [170] B. Liang, L. Fang, Y. Hu, G. Yang, Q. Zhu, X. Ye, *Nanoscale* **2014**, *6*, 4264.
- [171] Z. Lu, C. Mao, H. Zhang, *J. Mater. Chem. C* **2015**, *3*, 4265.
- [172] S. C. Narayanan, K. R. Karpagam, A. Bhattacharyya, *Fibers Polym.* **2015**, *16*, 1269.
- [173] S. Rana, T. Carvalho, R. Fangueiro, P. Vidinha, *Polym. Adv. Technol.* **2013**, *24*, 191.
- [174] B.-M. Min, G. Lee, S. H. Kim, Y. S. Nam, T. S. Lee, W. H. Park, *Biomaterials* **2004**, *25*, 1289.
- [175] M. Kang, H. J. Jin, *Colloid. Polym. Sci.* **2007**, *285*, 1163.
- [176] Y. Yang, X. L. Ding, T. Q. Zou, G. Peng, H. F. Liu, Y. B. Fan, *RSC Adv.* **2017**, *7*, 7954.
- [177] S. Aznar-Cervantes, M. I. Roca, J. G. Martinez, L. Meseguer-Olmo, J. L. Cenis, J. M. Moraleda, T. F. Otero, *Bioelectrochemistry* **2012**, *85*, 36.
- [178] O. S. Makin, L. C. Serpell, *FEBS J.* **2005**, *272*, 5950.
- [179] R. Tycko, *Q. Rev. Biophys.* **2006**, *39*, 1.
- [180] C. Meier, I. Lifincev, M. E. Welland, *Biomacromolecules* **2015**, *16*, 558.
- [181] M. Hamedi, A. Herland, R. H. Karlsson, O. Inganäs, *Nano Lett.* **2008**, *8*, 1736.
- [182] F. G. Backlund, A. Elfving, C. Musumeci, F. Ajjan, V. Babenko, W. Dzwolak, N. Solin, O. Inganäs, *Soft Matter* **2017**, *13*, 4412.
- [183] L. Altamura, C. Horvath, S. Rengaraj, A. Rongier, K. Elouarzaki, C. Gondran, A. L. B. Maçon, C. Vendrely, V. Bouchiat, M. Fontecave, D. Mariolle, P. Rannou, A. Le Goff, N. Duraffourg, M. Holzinger, V. Forge, *Nat. Chem.* **2017**, *9*, 157.
- [184] T. L. Lowe, A. Strzelec, L. L. Kiessling, R. M. Murphy, *Biochemistry* **2001**, *40*, 7882.
- [185] L. O. Tjernberg, J. Naslund, F. Lindqvist, J. Johansson, A. R. Karlstrom, J. Thyberg, L. Terenius, C. Nordstedt, *J. Biol. Chem.* **1996**, *271*, 8545.
- [186] M. J. Krysmann, V. Castelletto, A. Kelarakis, I. W. Hamley, R. A. Hule, D. J. Pochan, *Biochemistry* **2008**, *47*, 4597.
- [187] M. Amit, S. Appel, R. Cohen, G. Cheng, I. W. Hamley, N. Ashkenasy, *Adv. Funct. Mater.* **2014**, *24*, 5873.
- [188] M. Amit, G. Cheng, I. W. Hamley, N. Ashkenasy, *Soft Matter* **2012**, *8*, 8690.
- [189] M. Amit, N. Ashkenasy, *Isr. J. Chem.* **2014**, *54*, 703.
- [190] O. Silberbush, M. Amit, S. Roy, N. Ashkenasy, *Adv. Funct. Mater.* **2017**, *27*, 1604624.
- [191] D. Ivnitski, M. Amit, O. Silberbush, Y. Atsmon-Raz, J. Nanda, R. Cohen-Luria, Y. Miller, G. Ashkenasy, N. Ashkenasy, *Angew. Chem.* **2016**, *128*, 10142.
- [192] H. Xu, A. K. Das, M. Horie, M. S. Shaik, A. M. Smith, Y. Luo, X. Lu, R. Collins, S. Y. Liem, A. Song, P. L. A. Popelier, M. L. Turner, P. Xiao, I. A. Kinloch, R. V. Ulijn, *Nanoscale* **2010**, *2*, 960.
- [193] R. C. G. Creasey, Y. Shingaya, T. Nakayama, *Mater. Chem. Phys.* **2015**, *158*, 52.
- [194] L. L. del Mercato, P. P. Pompa, G. Maruccio, A. D. Torre, S. Sabella, A. M. Tamburro, R. Cingolani, R. Rinaldi, *Proc. Natl. Acad. Sci. USA* **2007**, *104*, 18019.
- [195] K. Besar, H. A. M. Ardoña, J. D. Tovar, H. E. Katz, *ACS Nano* **2015**, *9*, 12401.
- [196] H. A. M. Ardoña, J. D. Tovar, *Chem. Sci.* **2015**, *6*, 1474.
- [197] A. M. Sanders, T. J. Dawidczyk, H. E. Katz, J. D. Tovar, *ACS Macro Lett.* **2012**, *1*, 1326.
- [198] H. A. M. Ardoña, E. R. Draper, F. Citossi, M. Wallace, L. C. Serpell, D. J. Adams, J. D. Tovar, *J. Am. Chem. Soc.* **2017**, *139*, 8685.
- [199] A. M. Sanders, T. J. Magnanelli, A. E. Bragg, J. D. Tovar, *J. Am. Chem. Soc.* **2016**, *138*, 3362.
- [200] R. H. Tredgold, R. C. Sproule, J. McCanny, *J. Chem. Soc., Faraday Trans. 1* **1976**, *72*, 509.
- [201] D. D. Ordinario, L. Phan, J.-M. Jocsón, T. Nguyen, A. A. Gorodetsky, *APL Mater.* **2015**, *3*, 014907.
- [202] D. D. Ordinario, L. Phan, W. G. Walkup Iv, J.-M. Jocsón, E. Karshalev, N. Hüsken, A. A. Gorodetsky, *Nat. Chem.* **2014**, *6*, 596.
- [203] D. D. Ordinario, L. Phan, W. G. Walkup Iv, Y. Van Dyke, E. M. Leung, M. Nguyen, A. G. Smith, J. Kerr, M. Naeim, I. Kymissis, A. A. Gorodetsky, *RSC Adv.* **2016**, *6*, 57103.
- [204] D. D. Ordinario, L. Phan, Y. Van Dyke, T. Nguyen, A. G. Smith, M. Nguyen, N. M. Mofid, M. K. Dao, A. A. Gorodetsky, *Chem. Mater.* **2016**, *28*, 3703.
- [205] G. Wu, P. Feng, X. Wan, L. Zhu, Y. Shi, Q. Wan, *Sci. Rep.* **2016**, *6*, 23578.
- [206] N. Amdursky, X. Wang, P. Meredith, D. D. C. Bradley, M. M. Stevens, *Adv. Mater.* **2016**, *28*, 2692.
- [207] N. Amdursky, X. Wang, P. Meredith, D. J. Riley, D. J. Payne, D. D. C. Bradley, M. M. Stevens, *Adv. Mater.* **2017**, *29*, 1700810.
- [208] S. Pirbadian, M. Y. El-Naggar, *Phys. Chem. Chem. Phys.* **2012**, *14*, 13802.
- [209] M. Breuer, K. M. Rosso, J. Blumberger, *Proc. Natl. Acad. Sci. USA* **2014**, *111*, 611.
- [210] M. L. Tran, B. J. Powell, P. Meredith, *Biophys. J.* **2006**, *90*, 743.
- [211] E. Di Mauro, O. Carpentier, S. I. Yanez Sanchez, N. Ignoumba Ignoumba, M. Lalancette-Jean, J. Lefebvre, S. Zhang, C. F. O. Graeff, F. Cicoira, C. Santato, *J. Mater. Chem. C* **2016**, *4*, 9544.
- [212] M. Ambrico, P. F. Ambrico, T. Ligonzo, A. Cardone, S. R. Cicco, A. Lavizzera, V. Augelli, G. M. Farinola, *Appl. Phys. Lett.* **2012**, *100*, 253702.
- [213] S. Bravina, P. Lutsyk, A. Verbitsky, N. Morozovsky, *Mater. Res. Bull.* **2016**, *80*, 230.
- [214] Y. J. Kim, W. Wu, S.-E. Chun, J. F. Whitacre, C. J. Bettinger, *Proc. Natl. Acad. Sci. USA* **2013**, *110*, 20912.
- [215] A. B. Mostert, K. J. Davy, J. L. Ruggles, B. J. Powell, I. R. Gentle, P. Meredith, *Langmuir* **2009**, *26*, 412.
- [216] A. B. Mostert, S. B. Rienecker, C. Noble, G. R. Hanson, P. Meredith, *Sci. Adv.* **2018**, *4*, eaq1293.
- [217] E. Di Mauro, R. Xu, G. Soliveri, C. Santato, *MRS Commun.* **2017**, *7*, 141.
- [218] B. Szpoganicz, S. Gidanian, P. Kong, P. Farmer, *J. Inorg. Biochem.* **2002**, *89*, 45.
- [219] W. Osak, K. Tkacz-Śmiech, M. Elbanowski, J. Sławiński, *J. Biol. Phys.* **1995**, *21*, 51.
- [220] I. Mihai, F. Addiégo, D. Del Frari, J. Bour, V. Ball, *Colloids Surf., A* **2013**, *434*, 118.
- [221] T. Eom, K. Woo, W. Cho, J. E. Heo, D. Jang, J. I. Shin, D. C. Martin, J. J. Wie, B. S. Shim, *Biomacromolecules* **2017**, *18*, 1908.
- [222] L. Migliaccio, S. Aprano, L. Iannuzzi, M. G. Maglione, P. Tassini, C. Minarini, P. Manini, A. Pezzella, *Adv. Electron. Mater.* **2017**, *3*.
- [223] Y. Lin, Y. Li, X. Zhan, *Chem. Soc. Rev.* **2012**, *41*, 4245.
- [224] G. Yu, J. Gao, J. C. Hummelen, F. Wudl, A. J. Heeger, *Science* **1995**, *270*, 1789.
- [225] A. Mishra, P. Bäuerle, *Angew. Chem., Int. Ed.* **2012**, *51*, 2020.
- [226] J. Zhao, Y. Li, G. Yang, K. Jiang, H. Lin, H. Ade, W. Ma, H. Yan, *Nat. Energy* **2016**, *1*, 15027.
- [227] Efficiency plot of photovoltaic cells, <https://www.nrel.gov/pv/assets/images/efficiency-chart.png> (accessed: April 2018).
- [228] R. H. Friend, R. W. Gymer, A. B. Holmes, J. H. Burroughes, R. N. Marks, C. Taliani, D. D. C. Bradley, D. A. D. Santos, J. L. Brédas, M. Lögdlund, W. R. Salaneck, *Nature* **1999**, *397*, 121.

- [229] P. T. Chou, Y. Chi, *Chem. Eur. J.* **2007**, *13*, 380.
- [230] M. C. Gather, A. Kohnen, K. Meerholz, *Adv. Mater.* **2011**, *23*, 233.
- [231] M. A. Hickner, H. Ghassemi, Y. S. Kim, B. R. Einsla, J. E. McGrath, *Chem. Rev.* **2004**, *104*, 4587.
- [232] Y. Wang, K. S. Chen, J. Mishler, S. C. Cho, X. C. Adroher, *Appl. Energy* **2011**, *88*, 981.
- [233] H. Zhang, P. K. Shen, *Chem. Rev.* **2012**, *112*, 2780.
- [234] G. A. Snook, P. Kao, A. S. Best, *J. Power Sources* **2011**, *196*, 1.
- [235] P. Meredith, *US Patent 10/491,224*, **2004**.
- [236] C. J. Bettinger, J. F. Whitacre, Y. J. Kim, *US Patent 14/827,223*, **2016**.
- [237] P. Kumar, E. Di Mauro, S. Zhang, A. Pezzella, F. Soavi, C. Santato, F. Ciccoira, *J. Mater. Chem. C* **2016**, *4*, 9516.
- [238] S.-K. Kim, Y. K. Kim, H. Lee, S. B. Lee, H. S. Park, *ChemSusChem* **2014**, *7*, 1094.
- [239] H. Wang, Y. Yang, L. Guo, *Adv. Energy Mater.* **2017**, *7*, 1700663.
- [240] M. Ambrico, A. Cardone, T. Ligonzo, V. Augelli, P. F. Ambrico, S. Cicco, G. M. Farinola, M. Filannino, G. Perna, V. Capozzi, *Org. Electron.* **2010**, *11*, 1809.
- [241] N. Amdursky, G. Shalev, A. Handelman, S. Litsyn, A. Natan, Y. Roizin, Y. Rosenwaks, D. Szwarcman, G. Rosenman, *APL Mater.* **2013**, *1*, 062104.
- [242] H. Wang, F. Meng, Y. Cai, L. Zheng, Y. Li, Y. Liu, Y. Jiang, X. Wang, X. Chen, *Adv. Mater.* **2013**, *25*, 5498.
- [243] A. Jonsson, T. A. Sjöström, K. Tybrandt, M. Berggren, D. T. Simon, *Sci. Adv.* **2016**, *2*, e1601340.
- [244] T. Arbring Sjöström, M. Berggren, E. O. Gabrielsson, P. Janson, D. J. Poxson, M. Seitaniidou, D. T. Simon, *Adv. Mater. Technol.* **2018**, 1700360.
- [245] D. Khodagholy, J. N. Gelinias, Z. Zhao, M. Yeh, M. Long, J. D. Greenlee, W. Doyle, O. Devinsky, G. Buzsáki, *Sci. Adv.* **2016**, *2*, e1601027.
- [246] D. Khodagholy, J. N. Gelinias, G. Buzsáki, *Science* **2017**, *358*, 369.
- [247] C. J. Bettinger, J. P. Bruggeman, A. Misra, J. T. Borenstein, R. Langer, *Biomaterials* **2009**, *30*, 3050.
- [248] M. Sytnyk, M. Jakešová, M. Litviňuková, O. Mashkov, D. Kriegner, J. Stangl, J. Nebesářová, F. W. Fecher, W. Schöfberger, N. S. Sariciftci, *Nat. Commun.* **2017**, *8*, 91.
- [249] J. Rivnay, P. Leleux, M. Ferro, M. Sessolo, A. Williamson, D. A. Koutsouras, D. Khodagholy, M. Ramuz, X. Strakosas, R. M. Owens, *Sci. Adv.* **2015**, *1*, e1400251.
- [250] K. Tybrandt, E. O. Gabrielsson, M. Berggren, *J. Am. Chem. Soc.* **2011**, *133*, 10141.
- [251] D. Carrad, A. Mostert, A. Ullah, A. Burke, H. J. Joyce, H. Tan, C. Jagadish, P. Krogstrup, J. Nygård, P. Meredith, *Nano Lett.* **2017**, *17*, 827.
- [252] S. Nizamoglu, M. C. Gather, M. Humar, M. Choi, S. Kim, K. S. Kim, S. K. Hahn, G. Scarcelli, M. Randolph, R. W. Redmond, *Nat. Commun.* **2016**, *7*, 10374.
- [253] M. Kim, H. S. Kim, M. A. Kim, H. Ryu, H. J. Jeong, C. M. Lee, *Macromol. Biosci.* **2017**, *17*.
- [254] J. Rivnay, S. Inal, B. A. Collins, M. Sessolo, E. Stavrinidou, X. Strakosas, C. Tassone, D. M. Delongchamp, G. G. Malliaras, *Nat. Commun.* **2016**, *7*, 11287.
- [255] R. Balint, N. J. Cassidy, S. H. Cartmell, *Acta Biomater.* **2014**, *10*, 2341.
- [256] F. Pires, Q. Ferreira, C. A. Rodrigues, J. Morgado, F. C. Ferreira, *Biochim. Biophys. Acta, Gen. Subj.* **2015**, *1850*, 1158.
- [257] T. H. Qazi, R. Rai, A. R. Boccaccini, *Biomaterials* **2014**, *35*, 9068.
- [258] D. Mawad, C. Mansfield, A. Lauto, F. Perbellini, G. W. Nelson, J. Tonkin, S. O. Bello, D. J. Carrad, A. P. Micolich, M. M. Mahat, J. Furman, D. Payne, A. R. Lyon, J. J. Gooding, S. E. Harding, C. M. Terracciano, M. M. Stevens, *Sci. Adv.* **2016**, *2*, e1601007.
- [259] Y. Wu, Y. X. Chen, J. Yan, D. Quinn, P. Dong, S. W. Sawyer, P. Soman, *Acta Biomater.* **2016**, *33*, 122.
- [260] C. Cui, N. Faraji, A. Lauto, L. Travagliani, J. Tonkin, D. Mahns, E. Humphrey, C. Terracciano, J. J. Gooding, J. Seidel, D. Mawad, *Biomater. Sci.* **2018**, *6*, 493.
- [261] D. Xu, L. Fan, L. Gao, Y. Xiong, Y. Wang, Q. Ye, A. Yu, H. Dai, Y. Yin, J. Cai, L. Zhang, *ACS Appl. Mater. Interfaces* **2016**, *8*, 17090.
- [262] R. A. MacDonald, B. F. Laurenzi, G. Viswanathan, P. M. Ajayan, J. P. Stegemann, *J. Biomed. Mater. Res., Part A* **2005**, *74*, 489.
- [263] M. Li, Y. Guo, Y. Wei, A. G. MacDiarmid, P. I. Lelkes, *Biomaterials* **2006**, *27*, 2705.
- [264] J. H. Collier, J. P. Camp, T. W. Hudson, C. E. Schmidt, *J. Biomed. Mater. Res., Part A* **2000**, *50*, 574.
- [265] L. Ghasemi-Mobarakeh, M. P. Prabhakaran, M. Morshed, M. H. Nasr-Esfahani, S. Ramakrishna, *Tissue Eng., Part A* **2009**, *15*, 3605.
- [266] A. M. Martins, G. Eng, S. G. Caridade, J. o. F. Mano, R. L. Reis, G. Vunjak-Novakovic, *Biomacromolecules* **2014**, *15*, 635.
- [267] S. R. Shin, S. M. Jung, M. Zalabany, K. Kim, P. Zorlutuna, S. b. Kim, M. Nikkhah, M. Khabiry, M. Azize, J. Kong, K.-t. Wan, T. Palacios, M. R. Dokmeci, H. Bae, X. Tang, A. Khademhosseini, *ACS Nano* **2013**, *7*, 2369.
- [268] C.-C. Hsu, A. Serio, N. Amdursky, C. Besnard, M. M. Stevens, *ACS Appl. Mater. Interfaces* **2018**, *10*, 5305.
- [269] R. I. Pinhasi, D. Kallmann, G. Saper, H. Dotan, A. Linkov, A. Kay, V. Liveanu, G. Schuster, N. Adir, A. Rothschild, *Nat. Commun.* **2016**, *7*, 12552.
- [270] J. Barber, P. D. Tran, *J. R. Soc., Interface* **2013**, *10*, 20120984.
- [271] É. Boulais, N. P. D. Sawaya, R. Veneziano, A. Andreoni, J. L. Banal, T. Kondo, S. Mandal, S. Lin, G. S. Schlau-Cohen, N. W. Woodbury, H. Yan, A. Aspuru-Guzik, M. Bathe, *Nat. Mater.* **2017**, *17*, 159.
- [272] J. Lerner Yardeni, M. Amit, G. Ashkenasy, N. Ashkenasy, *Nanoscale* **2016**, *8*, 2358.